Authors responses

Moa K. Sporre[1,2], Sara M. Blichner[1], Roland Schrödner[3], Inger H. H. Karset[1], Terje K. Berntsen[1,4], Twan van Noije[5], Tommi Bergman[5,6], Declan O'Donnell[6], and Risto Makkonen[6,7]

[1]Department of Geosciences, University of Oslo, Postboks 1022 Blindern, 0315 Oslo, Norway
[2]Now at: Department of Physics, Lund University, Box 118, 22100 Lund, Sweden
[2]Institute for Tropospheric Research, Permoserstr. 15, 04318 Leipzig, Germany
[4]CICERO Center for International Climate Research, Postboks 1129 Blindern, 0318 Oslo, Norway
[5]Royal Netherlands Meteorological Institute (KNMI), PO Box 201, 3730 AE De Bilt, the Netherlands
[6]Climate System Research, Finnish Meteorological Institute, P.O. Box 503, FI-00101, Helsinki, Finland
[7]Institute for Atmospheric and Earth System Research / Physics, Faculty of Science, University of Helsinki, P.O. Box 64, FI-00014, Finland

We would like to thank the reviewers for their comments which will improve this manuscript. We present our responses to the questions and comments below. The comments from the reviewer are written first and our responses follow in italic. We will answer the comments from all three referees in this document.

Reviewer number 1

Line 360: Why does increase in accumulation mode particles over remote regions cause a decrease in smaller (20-60 nm) particles in this model? If SOA gas precursors are transported to remote regions they should be effective in growing 20-60 nm particles to CCN sizes. This should increase CCN, CDNC and CRE. But it seems the opposing effects on accumulation and Aitken particles is related to transport of already formed accumulation mode SOA (upstream of the remote regions) that decreases smaller (20-60 nm) particles due to coagulation?

We agree with the reviewer that transport of already formed accumulation mode particles is a plausible explanation for the change in the size distributions over the remote regions. With the model output we have we can however not confirm that this is the explanation.

Conceptually, if in EC-Earth the timescale for SOA formation could increase by reducing oxidants over remote regions (due to changes in gas-phase chemistry), this should increase CCN?

Yes. The effect has also been seen in other models (e.g. Karset et al., 2018).

Line 395: The strong reduction in nucleation rates in EC-Earth over large anthropogenic regions (due to shutting off ELVOCs) seems less realistic. BL nucleation rates should not be shut off when ELVOCs are zero. Observational evidence suggests that presence of H2SO4 will nucleate particles while low volatility organics grow these particles to CCN sizes (e.g. Riipinen et al. 2011 cited in this paper). Please comment on how realistic the nucleation rates are in EC-Earth based on observational evidence.

We agree with the reviewer that completely shutting off the boundary layer nucleation when ELVOCs are zero is not a very realistic. However, the complete absence of ELVOCs is a sensitivity test and not a very likely scenario. The nucleation rate parameterization in EC-Earth is based on the experiments from the CLOUD chamber and has performed well in other models when compared to measurements (Riccobono et al., 2014). However, the nucleation rates in EC-Earth may be underestimated over oceans since there are no VOC emissions from the ocean in this model in these simulations.

Line 425: Why does increase in OH in EC-Earth (in no isoprene) cause reduction in O3?

Since O_3 is produced when isoprene is oxidised. We have changed this text to make this clear and it now reads: "The concentration of O_3 is reduced since the oxidation of of isoprene results in the production of O_3. However, the loss rate of MT to O_3 oxidation is less important than OH, and thus the overall result is a reduction in column burden."

Line 425: Why does increase in oxidants not affect amount of SOA formed? If more SOA is formed close to sources it can undergo wet removal. Also dry deposition of SOA precursors would reduce available precursors. This could also change if SOA precursors L/SVOCs and their multigenerational chemistry are represented by a volatility basis set framework. For example see: https://agupubs.onlinelibrary.wiley.com/doi/10.1002/2014JD022563.

The ELVOC and L/SVOCs in these three models do not undergo any wet or dry deposition. Therefore, all formed ELVOC and L/SVOCs will form SOA eventually. How close to the sources this will occur depends on the available oxidants in EC-Earth. We agree with the reviewer that this would not occur if a volatility basis set framework would have been used in the models.

Line 495-505: It is clear that the three global models would produce different results if used to investigate climate impacts of BVOCs. But observations could provide insights about changes in model behavior with respect to changes in VOC emissions, NPF, presence/absence of ELVOCs and H2SO4. Also one of the key insights from this work is importance of interactive oxidants. Future model measurement comparisons could focus on evaluating model responses to perturbations in VOC emissions, NPF, SO2, NOx emissions etc. with respect to observations for e.g. in cleaner locations such as over the Amazon: https://www.nature.com/articles/s41467-019-08909-4

We agree that comparing the models to measurements is important, though out of the scope of this manuscript. A comment regarding model evaluation has been added to the further discussions section.

Minor clarification comments: Page 2: Shrivastava et al. 2015 predicted biomass burning to be the largest SOA source followed by biogenic SOA. Fossil-fuel SOA burden was the smallest and contributed less than one-third of biogenic SOA (see their Figure 5). Please rephrase.

Yes, this has been corrected.

Sum of isoprene, monoterpene and sesquiterpene emissions to BVOCs should sum to 100%. Right now 50+15+3 is 68%. Am I missing something here?

The rest of the emitted BVOC compounds (32 %) are not as relevant for aerosol formation (e.g. methanol, acetone, CO etc). We have changed the text to make this clear. The sentence now reads: "However, in ESMs these are often reduced to be represented by 2-3 tracers, usually isoprene, monoterpenes (MTs) and sesquiterpenes which constitute the main contributors to aerosol formation and are estimated to constitute around 50%, 15% and 3% respectively of the total BVOC emissions [...]"

Line 270-275: Why does ECHAM have more particles in nucleation mode than EC-Earth? Does EC-Earth treat nucleation mode? I would expect since NorESM has no nucleation mode, it would have the lowest particle numbers since the SOA mass goes to larger particles, but seems EC-Earth has the lowest numbers. Why?

One of the reasons why ECHAM has more particles in the nucleation mode is the diameter at which the newly formed particles are introduced to this mode. This diameter is lower than the nucleation mode median in ECHAM which means that the mode median is reduced when there is new particle formation. This reduces the amount of particles that are transferred to the Aitken mode which means more particles are left in the nucleation mode in ECHAM. This does not occur in EC-Earth because here the diameter of the newly formed particles is above the mode median. We write about this in the discussion. Another explanation for the large difference between the nucleation modes in EC-Earth and ECHAM could be that the nucleation rates in ECHAM might be overestimated. Moreover, the nucleation rates over the oceans in EC-Earth may be underestimated as described in an earlier comment.

There are most likely many different reasons to why EC-Earth has lower particle concentrations than NorESM. One possible explanation could be higher wet deposition in EC-Earth due to a 6 hour coupling time step between TM5 and IFS. This means that it can rain for 6 hours in a row in TM5. The difference in the aerosol size distributions can also be linked to how the emissions (which are mass based) are partitioned into the different size modes, which is different in the models.

We have added the following sentences to the manuscript to address these questions: "There are likely many different explanations to why the size distributions and aerosol number concentrations are different in the models. Some plausible explanations include differences in wet deposition, nucleation rates and how the emissions in general are partitioned into the aerosol modes."

Line 285: I would think if aerosols are located above bright/reflective surfaces, they will absorb more sunlight and contribute more strongly to DRE. But it seems in NorESM when there is higher AOD above bright surfaces it results in lower DRE forcing. Above deserts, dust particles should also be light absorbing. So this statement is confusing.

Please explain.

The high AOD over deserts in NorESM is mainly a result of high desert dust emissions. These aerosols are mainly reflecting incoming solar radiation and not absorbing very much. Reflective aerosols above a light surface (such as deserts) have almost the same properties as the surface below and therefore only have a modest radiative effect. We have added a sentence to the manuscript explaining that the high AOD over desserts in NorESM is associated with large dust emissions.

Also how do the various models determine fraction going to soluble versus insoluble modes?

Emissions are partitioned between soluble/insoluble modes in fixed proportions. E.g. in TM5 it is assumed that all carbona-

ceous aerosol from sources other than biofuel burning and open biomass burning to be emitted as insoluble (into the Aitken mode). Insoluble particles are aged through condensation of sulfuric acid, and when coated with H_2SO_4, are transferred to the corresponding soluble size mode. Coagulation of insoluble and soluble particles also results in soluble particles.

Is hygroscopicity of insoluble mode assumed to be zero?
Yes, in both EC-Earth and ECHAM.

What is assumed hygroscopicity of SOA in soluble/insoluble modes and in different models? I would expect hygroscopicity of SOA to play a stronger role in SOA dominated regions like the Amazon. Please comment on the role of hygroscopicity and water uptake on aerosol-cloud-radiation interactions.
The hygroscopicity parameter for organic aerosols (including SOA) in NorESM is 0.14 (Kirkevåg et al., 2018). The kappa for soluble organic aerosols in EC-Earth in terms of cloud activation is 0.1 and the kappa for organics in ECHAM is 0.06. For the insoluble mode see the previous question. There is a sentence addressing hygroscospicity included in Section 3.2.2. of the manuscript.

Why does EC-Earth experience particle number changes farther downstream related to other models? Is it related to interactive oxidants in this model that reduce SOA formation close to sources but increase it downwind relative to a model with prescribed oxidants?
Yes, we consider this a plausible explanation. We have added a paragraph to the discussions section where we discuss the interactive oxidants a bit more extensively.

Line 335: It says “smaller” CWP due to higher CCN, CDNC and smaller effective radius. I think the authors meant “larger” CWP?
This is correct. We have changed "smaller" to "larger" in the text.

Reviewer number 2

I suggest the authors discuss/compare not only with the Tsigaridis et al (2014) paper on organic aerosols but also with the Fanourgakis et al (2019) on CCN, where several models with different treatment of NPF and of OA have been compared. How the SOA budget calculated in this study compare with the earlier estimates reported in both the above mentioned papers. How the aerosol number concentrations and the CCN calculated compare with Fanourgakis et al. What do we learn from comparison with these earlier studies?
We have added a comparison to the Tsigaridis et al. (2014) study. We have read the Fanourgakis et al (2019) very carefully and though it is a very interesting paper we find it hard to make comparison between the results from that study and this manuscript. In terms of SOA budget, the Fanourgakis et al (2019) study uses OA concentrations which is not a parameter that we have investigated in this study. Moreover, we have not included results regarding CCN concentrations in this study and

can therefore not compare these concentrations to those in Fanourgakis et al (2019). Both studies include aerosol number concentrations above 3 nm but Fanourgakis et al (2019) uses near-surface concentrations while we used average values at pressure above 850 hPa. Since the concentrations of particles changes rapidly in the lowermost layers of the models we do not see it fit to compare these concentrations either. However, studies where models are compared to measurements are of great importance in developing models and we have added a comment to emphasize this in the discussion.

Furthermore, I would like to see some conclusive discussion on the importance of the interactive calculations of the oxidants (only EC-Earth having this feature) and shows very different behavior compared to the other two ESMs for the simulations without biogenic VOCs, pointing to potentially some chemical feedback mechanisms though oxidants impact on SOA formation that is not discussed. *We have added a paragraph to the Further discussions section where we discuss the interactive oxidants in EC-Earth further.*

Extra specific comments: 1- Line 45: Kanakidou et al. (2000) and Carlton et al (2008) have discussed the anthropogenic control on BSOA before Spracklen et al. (2011) I think they deserve citation here. *We have added these two references here.*

2- Lines 60-62: Assumption of irreversible condensation of organics is a working assumption for ELVOC but not for SVOC. I think this has to be discussed here since for SVOC this will lead to an overestimate of SOA formation. *We have added a paragraph to the discussion where we include a discussion on the irreversible condensation of SVOCs.*

3- Lines 129 Table 1: The model description leaves the impression to the reader that MEGAN is used on line in all three ESMs while in Table 1 it is stated that two among the three ESMs use recalculated fields. This has to be clarified.
MEGAN has been used to calculate the emissions for all three models. However, for two of the models this had been done offline and these are denoted prescribed in the table. We have rewritten the text in the methods section such that it now reads: "Moreover, all three ESMs use the Model of Emissions of Gases and Aerosols from Nature (MEGAN) version 2.1 (Guenther et al., 2012). However, in NorESM, MEGAN is run interactively while the other two models use emissions produced in offline simulations with MEGAN."

Reviewer number 3

Although the paper is generally well written, I think the caveats and conclusions need to reflect some of the issues which this study couldn't address. I actually disagree with the last line of the conclusions which says that "in particular" one needs to work more on how NPF parameterizations affect size distributions. Although I agree that these NPF issues are important, I don't see the evidence that this is the main problem with SOA modeling. I suspect it reflects more the author's plans and interests than the general level of SOA understanding.
We have added a paragraph in the further discussions section where we address limitations of these models. This investigation does not investigate how important these NPF issues are in comparison to other uncertainties regarding SOA and we do not

make any such conclusions. Our view is that the NPF issues is not competing with other SOA modelling issues but is rather a part of the overall uncertainty regarding SOA impact on climate. Nevertheless, we have removed the words "in particular" from the last sentence.

A few connected issues are:

The authors clearly state that their semi-volatile SOA compounds aren't semi-volatile - they are formed as inert and condensed species upon BVOC oxidation. This is a major assumption, but the implications are not discussed anywhere in the manuscript. Compared to a true VBS equilibrium framework these models presumably give much more SOA in less polluted regions, and in the free troposphere. Isn't this one of the main uncertainties of all of these models?
We have added a paragraph to the discussion where we include a discussion on the irreversible condensation of SVOCs and the VBS equilibrium framework.

No model evaluation is presented, and no indication is given as to where such evaluations can be found. The model versions used here seem to differ from those used by Tsigaridis et al, 2014, so readers have no idea if the modelled SOA are reasonable or not.
We have added a sentence comparing the modelled SOA in this study to the results in Tsigaridis et al. (2014): "The produced SOA mass in the models are in the range of the values found in Tsigaridis et al. (2014) but are higher than the median of the models included in that study." However, a large model evaluation is beyond the scope of this manuscript.

There is no comparison of the BSOA production calculated here with that of other studies, e.g. Hallquist et al 2009 or Tsigaridis et al. 2014.
The BSOA is included in the SOA production terms but we have not calculated this fraction explicitly in this study. Therefore we have not included a comparison of the BSOA separately in this paper.

Although the paper mentions the Spracklen et al 2011 study concerning anthropogenic influence (also commented below), there is no mention of the role of NOx on the BSOA yields assumed in this paper. Most VBS schemes would have both high and low NOx yields, and perform some interpolation between them depending on oxidant availability. If one believes in some anthropogenic influence, then the assumed yields should depend on NOx as well as oxidants.
The models used in this study have no yield dependence on NOx or oxidants. We have added a paragraph discussing SOA and the limitations of these models in terms of their SOA parametrisations to the discussion section.

I also missed any mention of POA, BBOA, or ASOA in Sect. 2 and elsewhere. Do these models only have BSOA? What are the implications of this?
We have added a paragraph discussing SOA and the limitations of these models in terms of their SOA parametrisations to the

discussion section. Here we discuss POA and ASOA. We do not know what BBOA is but we assume that the reviewer means BPOA, which is also discussed in the new paragraph.

Other issues

p1, L10. Why 10 years? The importance of BVOC to SOA formation has been known for decades!

We have removed "past 10". The sentence now reads: "As the understanding of the importance of BVOCs for aerosol formation has increased over the years these processes have made their way into Earth System Models (ESMs)"

p2, L1. Say implies rather than introduces

We have changed this according to the reviewer's comment.

p2, L5. Not all BVOC are "quickly" oxidized.

We have removed the word quickly.

p2, L10. Give reference for the direct aerosol effect comment

We have added a reference to (Charlson et al., 1990).

p2, L11. Add radiation as one of the major drivers of BVOC emissions

We have added radiation as one of the main drivers.

p2, L12. It is usually good to cite articles if possible, and could have used e.g. Hantson et al 2017 or Schurgers et al. 2009 here.

We added the Hantson et al. (2017) reference.

p2, L13. There are several studies suggesting that increased CO2 can inhibit BVOC emissions (e.g. Arneth et al, 2007, refs in Hantson et al 2017). This is also a major source of uncertainty that needs a mention.

We have added this sentence: "There are however a range of uncertainties associated with these feedbacks, including CO_2 inhibition of BVOC emissions (Arneth et al., 2007)."

p2, L22. Season matters. BSOA often dominates SOA in summertime, but there is plenty of evidence that in wintertime wood-burning often dominates or plays a major role (e.g. Brown et al., 2016, Glasius et al., 2018).

A sentence has been added on regional and seasonal differences and we have included a reference to (Glasius et al., 2018). The new sentence reads: "However, there are large seasonal and regional differences in sources, with BSOA dominating in sum-

mer, while sources like wood burning can be more dominant in winter, in particular in populated regions (Glasius et al., 2018)."

p2, L24. Although the Spracklen et al 2011 study was very innovative and interesting, there are several issues with the conclusions, see e.g. Hodzic Jimenez, 2011. This question is very complex and unresolved as far as I know.
We have reworded this sentence somewhat and it now reads: "Moreover, some studies have found that the biogenic SOA formation is anthropogenically controlled (Spracklen et al., 2011; Kanakidou et al., 2000; Carlton et al., 2010)."

p3, L30-33. I think the sentences starting on L30 are very clear, fair, and with the important caveat represented by the last sentence. These lines could usefully be used in the abstract.
We have added the following sentence to the abstract: "The goal of the study is to investigate whether it is of importance to treat SOA formation processes correctly in the models, rather than to evaluate the correctness of the current treatment in the models."

p5, L2. The descriptions are brief, not "detailed".
We have added "more" before detailed to highlight that the descriptions in the next sections are more detailed than the brief description in this paragraph.

p5, L13. Which MEGAN version?
We have included "version 2.1" to the text to clarify this.

p6, L1. So, is this a new version of NorESM, or a version used just for this study? If the latter, then the conclusions aren't relevant to other NorESM work, which would seem to remove some of the point of including this model.
This is not a new version of the model, but a minor modification of it. This modification is included in future versions of the model so the results from this study are still relevant.

p6, L9. I think you mean hydroxyl, not hydroxide, and better to say nitrate radical, as nitrate is often used for the aerosol compound.
We have changed this according to the reviewer's suggestion.

p6, L11. This was confusing. If I understand right, one has two types of ELVOC then, one that can influence NPF, and the other behaves exactly as L/SVOC. As you ELVOC and L/SVOC compounds have the same mass, why not simply put the non-NPF ELVOC in as L/SVOC?
The idea behind type of parametrizing of the ELVOCs in NorESM is that not all VOC formed from the oxidation of monoterpene by ozone have low enough volatility to contribute to new particle formation (NPF). Therefore, only 50 %. of the ELVOCs can participate in NPF. The advantage of this treatment is that we essentially have three types of VOCs in NorESM but only two

tracers. This is not used in the version of the model used in this paper but has been utilized in new developments of the model.

p7, L32. This was also confusing. Table 1 suggests that ECHAM uses fixed yields of L/SVOC and ELVOC, but L32 suggests partitioning depends on pre-existing organic mass. And what is meant by pre-existing OM? Does this influence the DRE/CRE calculations?

The yields are fixed. The partitioning concerns the partitioning to the different aerosol modes. We have changed the text to clarify this and the text now reads: "The SOA formation mechanism (Jokinen et al., 2015) includes both kinetic condensation to Fuchs-corrected surface area (condensation sink). Moreover, the relative partitioning to the Aitken/accumulation/coarse mode is done according to pre-existing organic mass in the respective modes."

All organic mass is considered in the DRE/CRE calculations.

p9, L2-7. I am not sure the argument about interactive oxidants can explain a factor of 3. Sure, when the BVOC are emitted one can expect reduced OH and other oxidants, but this just delays the oxidation close to the surface. Isoprene which isn't oxidized near the surface will still be oxidized a little further up in the troposphere. Why would the total amount change by a factor of 3? Did you check changes in oxidant fields associated with this argument?

We have written in the article that this can partly be explained by the interactive oxidants and thus do not claim that the interactive oxidants can explain a factor of 3. If isoprene is oxidised further away from the sources it will increase the lifetime of the isoprene which also increases the column burden. Not only the average level of the oxidants but also the diurnal variation of the both BVOCs and oxidants and their timing will matter for the lifetime and of the BVOCs and affect how close to the sources they are oxidised. We have not compared the oxidant fields between the models since we don't have this output from all the models.

p16-17. This is where I think the limitations and results of this study need to be put alongside the many other uncertainties surrounding SOA modelling.

We have added a paragraph on limitations and uncertainties regarding the SOA parameterizaitons in the ESMs used in this study here.

p26, Fig. 1. State which years are shown here. Also, I was surprised to see no errorbars on the ECHAM runs, and that even those for NorESM were so small. Did ECHAM also just use one fixed year (2000) of BVOC emission, same as EC-Earth?

Yes, ECHAM uses the emissions from one fixed year. We have added information regarding this to the figure text.

References

Arneth, A., Niinemets, U., Pressley, S., Back, J., Hari, P., Karl, T., Noe, S., Prentice, I. C., Serca, D., Hickler, T., Wolf, A., and Smith, B.: Process-based estimates of terrestrial ecosystem isoprene emissions: incorporating the effects of a direct CO2-isoprene interaction, Atmospheric Chemistry and Physics, 7, 31–53, https://doi.org/10.5194/acpd-6-8011-2006, 2007.

Carlton, A. G., Pinder, R. W., Bhave, P. V., and Pouliot, G. A.: To What Extent Can Biogenic SOA be Controlled?, Environmental Science & Technology, 44, 3376–3380, https://doi.org/10.1021/es903506b, https://doi.org/10.1021/es903506b, pMID: 20387864, 2010.

Charlson, R. J., Langner, J., and Rodhe, H.: Sulphate aerosol and climate, Nature, 348, 22, https://doi.org/10.1038/348022a0, https://doi.org/10.1038/348022a0, 1990.

Glasius, M., Hansen, A. M. K., Claeys, M., Henzing, J. S., Jedynska, A. D., Kasper-Giebl, A., Kistler, M., Kristensen, K., Martinsson, J., Maenhaut, W., Nøjgaard, J. K., Spindler, G., Stenström, K. E., Swietlicki, E., Szidat, S., Simpson, D., and Yttri, K. E.: Composition and sources of carbonaceous aerosols in Northern Europe during winter, Atmospheric Environment, 173, 127–141, https://doi.org/10.1016/j.atmosenv.2017.11.005, http://www.sciencedirect.com/science/article/pii/S1352231017307471, 2018.

Guenther, A. B., Jiang, X., Heald, C. L., Sakulyanontvittaya, T., Duhl, T., Emmons, L. K., and Wang, X.: The model of emissions of gases and aerosols from nature version 2.1 (MEGAN2.1): An extended and updated framework for modeling biogenic emissions, Geoscientific Model Development, 5, 1471–1492, https://doi.org/10.5194/gmd-5-1471-2012, 2012.

Hantson, S., Knorr, W., Schurgers, G., Pugh, T. A., and Arneth, A.: Global isoprene and monoterpene emissions under changing climate, vegetation, CO2and land use, Atmospheric Environment, 155, 35–45, https://doi.org/10.1016/j.atmosenv.2017.02.010, http://dx.doi.org/10.1016/j.atmosenv.2017.02.010, 2017.

Jokinen, T., Berndt, T., Makkonen, R., Kerminen, V.-M., Junninen, H., Paasonen, P., Stratmann, F., Herrmann, H., Guenther, A. B., Worsnop, D. R., Kulmala, M., Ehn, M., and Sipilä, M.: Production of extremely low volatile organic compounds from biogenic emissions: Measured yields and atmospheric implications, Proceedings of the National Academy of Sciences, 112, 7123–7128, https://doi.org/10.1073/pnas.1423977112, http://www.pnas.org/lookup/doi/10.1073/pnas.1423977112, 2015.

Kanakidou, M., Tsigaridis, K., Dentener, F. J., and Crutzen, P. J.: Human-activity-enhanced formation of organic aerosols by biogenic hydrocarbon oxidation, Journal of Geophysical Research: Atmospheres, 105, 9243–9354, https://doi.org/10.1029/1999JD901148, https://agupubs.onlinelibrary.wiley.com/doi/abs/10.1029/1999JD901148, 2000.

Karset, I. H. H., Berntsen, T. K., Storelvmo, T., Alterskjær, K., Grini, A., Olivié, D., Kirkevåg, A., Seland, Ø., Iversen, T., and Schulz, M.: Strong impacts on aerosol indirect effects from historical oxidant changes, Atmospheric Chemistry and Physics, 18, 7669–7690, https://doi.org/10.5194/acp-18-7669-2018, https://www.atmos-chem-phys.net/18/7669/2018/, 2018.

Kirkevåg, A., Grini, A., Olivié, D., Seland, Ø., Alterskjær, K., Hummel, M., Karset, I. H. H., Lewinschal, A., Liu, X., Makkonen, R., Bethke, I., Griesfeller, J., Schulz, M., and Iversen, T.: A production-tagged aerosol module for earth system models, OsloAero5.3 – extensions and updates for CAM5.3-Oslo, Geoscientific Model Development, 11, 13 945–3982, https://doi.org/10.5194/gmd-11-3945-2018, 2018.

Riccobono, F., Schobesberger, S., Scott, C. E., Dommen, J., Ortega, I. K., Rondo, L., Almeida, J., Amorim, A., Bianchi, F., Breitenlechner, M., David, A., Downard, A., Dunne, E. M., Duplissy, J., Ehrhart, S., Flagan, R. C., Franchin, A., Hansel, A., Junninen, H., Kajos, M., Keskinen, H., Kupc, A., Kürten, A., Kvashin, A. N., Laaksonen, A., Lehtipalo, K., Makhmutov, V., Mathot, S., Nieminen, T., Onnela, A., Petäjä, T., Praplan, A. P., Santos, F. D., Schallhart, S., Seinfeld, J. H., Sipilä, M., Spracklen, D. V., Stozhkov, Y., Stratmann, F., Tomé, A., Tsagkogeorgas, G., Vaattovaara, P., Viisanen, Y., Vrtala, A., Wagner, P. E., Weingartner, E., Wex, H., Wimmer, D., Carslaw, K. S., Curtius, J., Donahue, N. M., Kirkby, J., Kulmala, M., Worsnop, D. R., and Baltensperger, U.: Oxidation Products of Biogenic Emissions Contribute

to Nucleation of Atmospheric Particles, Science, 344, 717–721, https://doi.org/10.1126/science.1243527, http://science.sciencemag.org/content/344/6185/717, 2014.

Spracklen, D. V., Jimenez, J. L., Carslaw, K. S., Worsnop, D. R., Evans, M. J., Mann, G. W., Zhang, Q., Canagaratna, M. R., Allan, J., Coe, H., McFiggans, G., Rap, A., and Forster, P.: Aerosol mass spectrometer constraint on the global secondary organic aerosol budget, Atmospheric Chemistry and Physics, 11, 12 109–12 136, https://doi.org/10.5194/acp-11-12109-2011, https://www.atmos-chem-phys.net/11/12109/2011/, 2011.

Tsigaridis, K., Daskalakis, N., Kanakidou, M., Adams, P. J., Artaxo, P., Bahadur, R., Balkanski, Y., Bauer, S. E., Bellouin, N., Benedetti, A., Bergman, T., Berntsen, T. K., Beukes, J. P., Bian, H., Carslaw, K. S., Chin, M., Curci, G., Diehl, T., Easter, R. C., Ghan, S. J., Gong, S. L., Hodzic, A., Hoyle, C. R., Iversen, T., Jathar, S., Jimenez, J. L., Kaiser, J. W., Kirkevåg, A., Koch, D., Kokkola, H., Lee, Y. H., Lin, G., Liu, X., Luo, G., Ma, X., Mann, G. W., Mihalopoulos, N., Morcrette, J.-J., Müller, J.-F., Myhre, G., Myriokefalitakis, S., Ng, N. L., O'Donnell, D., Penner, J. E., Pozzoli, L., Pringle, K. J., Russell, L. M., Schulz, M., Sciare, J., Seland, , Shindell, D. T., Sillman, S., Skeie, R. B., Spracklen, D., Stavrakou, T., Steenrod, S. D., Takemura, T., Tiitta, P., Tilmes, S., Tost, H., van Noije, T., van Zyl, P. G., von Salzen, K., Yu, F., Wang, Z., Wang, Z., Zaveri, R. A., Zhang, H., Zhang, K., Zhang, Q., and Zhang, X.: The AeroCom evaluation and intercomparison of organic aerosol in global models, Atmos. Chem. Phys., 14, 10 845–10 895, https://doi.org/10.5194/acp-14-10845-2014, https://www.atmos-chem-phys.net/14/10845/2014/, 2014.

Large difference in aerosol radiative effects from BVOC-SOA treatment in three ESMs

Moa K. Sporre[1,2], Sara M. Blichner[1], Roland Schrödner[3], Inger H. H. Karset[1], Terje K. Berntsen[1,4], Twan van Noije[5], Tommi Bergman[5,6], Declan O'Donnell[6], and Risto Makkonen[6,7]

[1]Department of Geosciences, University of Oslo, Postboks 1022 Blindern, 0315 Oslo, Norway
[2]Now at: Department of Physics, Lund University, Box 118, 22100 Lund, Sweden
[2]Institute for Tropospheric Research, Permoserstr. 15, 04318 Leipzig, Germany
[4]CICERO Center for International Climate Research, Postboks 1129 Blindern, 0318 Oslo, Norway
[5]Royal Netherlands Meteorological Institute (KNMI), PO Box 201, 3730 AE De Bilt, the Netherlands
[6]Climate System Research, Finnish Meteorological Institute, P.O. Box 503, FI-00101, Helsinki, Finland
[7]Institute for Atmospheric and Earth System Research / Physics, Faculty of Science, University of Helsinki, P.O. Box 64, FI-00014, Finland

Correspondence: Moa Sporre (moa.sporre@nuclear.lu.se)

Abstract. Biogenic volatile organic compounds (BVOCs) emitted from vegetation are oxidized in the atmosphere and can form aerosol particles either by contributing to new particle formation or by condensing onto existing aerosol particles. As the understanding of the importance of BVOCs for aerosol formation has increased over the ~~past 10~~ years these processes have made their way into Earth System Models (ESMs). In this study, sensitivity experiments are run with three different ESMs, (the Norwegian Earth System Model (NorESM), EC-Earth and ECHAM) to investigate how the direct and indirect aerosol radiative effects are affected by changes in the formation of secondary organic aerosol (SOA) from BVOCs. In the first two sensitivity model experiments, the yields of SOA precursors from oxidation of BVOCs are changed by ±50 %. For the third sensitivity test, the formed oxidation products do not participate in the formation of new particles, but are only allowed to condense onto existing aerosols. In the last two sensitivity experiments, the emissions of BVOC compounds (isoprene and monoterpenes) are turned off, one at a time. The goal of the study is to investigate whether it is of importance to treat SOA formation processes correctly in the models, rather than to evaluate the correctness of the current treatment in the models.

The results show that the impact on the direct radiative effect (DRE) are linked to the changes in the SOA production in the models, where more SOA leads to a stronger DRE and vice versa. The magnitude by which the DRE changes (maximally 0.15 Wm^{-2} globally averaged) in response to the SOA changes however varies between the models, with EC-Earth displaying the largest changes. The results for the cloud radiative effects (CRE) are more complicated than for the DRE. The changes in CRE differ more among the ESMs and for some sensitivity experiments they even have different signs. The most sensitive models are NorESM and EC-Earth, which has CRE changes of up to 0.82 Wm^{-2}. The varying responses in the different models are connected to where in the aerosol size distributions the changes in mass and number due to SOA formation occur, in combination with the aerosol number concentration levels in the models. We also find that interactive gas-phase chemistry as well as the new particle formation parameterization have important implications for the DRE and CRE in some of the sensitivity experiments. The results from this study indicate that BVOC-SOA treatment in ESMs can have a substantial impact on the

modelled climate but that the sensitivity varies greatly between the models. Since BVOC emissions have changed historically and will continue to change in the future, the spread in model results found in this study ~~introduces~~ implies uncertainty into ESM estimates of aerosol forcing from land-use change and BVOC feedback strengths.

1 Introduction

The climatic relevance of biogenic volatile organic compounds (BVOCs) emitted from vegetation has received increasing attention over the past years. Emitted BVOCs are ~~quickly~~ oxidized in the atmosphere producing a number of different products with lower volatility. These can then form secondary organic aerosols (SOA), increasing both aerosol number concentration (through new particle formation (NPF), and participation in early growth) and aerosol sizes (through condensation onto pre-existing particles) (Shrivastava et al., 2017). The formation of SOA from BVOCs can thus influence climate both through changes in cloud properties (indirect aerosol effects) (Twomey, 1974; Albrecht, 1989) and through changes in scattering and absorption of solar radiation by aerosols (direct aerosol effect) (Charlson et al., 1990).

BVOC emissions depend on various environmental factors, in particular temperature, radiation, CO_2 concentrations and land use and are thus expected to have changed in the past and to continue to change in the future ~~(e.g. Bonan, 2016, sec. 31.6)~~ (e.g. Bonan, 2016; Hantson et al., 2017). Studies have found that future BVOC emissions are likely to increase due to warming and higher CO_2 concentrations, and that BVOCs could dampen temperature increase and provide a negative climate feedback (Sporre et al., 2019; Paasonen et al., 2013; Kulmala et al., 2014; Scott et al., 2018; Carslaw et al., 2010). ~~It is thus~~ There are however a range of uncertainties associated with these feedbacks, including the strength of CO_2 inhibition on BVOC emissions (Arneth et al., 2007). It is however important to include these processes in Earth System Models (ESMs) to estimate aerosol effects in the future, but also in the past. SOA formation has been added to many models over the recent years in response to the increased understanding of the importance of BVOCs to aerosol formation. However, uncertainties regarding these processes in models are large, e.g. Tsigaridis et al. (2014a) show an order of magnitude variation between the 31 models in the vertical profile of organic aerosol mass in their intercomparison.

Organics constitute a large fraction of the atmospheric aerosol mass (Shrivastava et al., 2017; Zhang et al., 2007) and as much as 50-85 % of this can be SOA (Zhang et al., 2007; Glasius and Goldstein, 2016). In model estimates, biogenic SOA usually dominates the SOA budget (Glasius and Goldstein, 2016; Hallquist et al., 2009; Kelly et al., 2018). As an exception, Shrivastava et al. (2015) find biomass ~~and fossil fuel~~ burning to be the largest source, and biogenics to be the second largest. ~~Moreover, Spracklen et al. (2011) claim~~ However, there are large seasonal and regional differences in sources, with BSOA dominating in summer, while sources like wood burning can be more dominant in winter, in particular in populated regions (Glasius et al., 2018). Moreover, some studies have found that the biogenic SOA formation is anthropogenically controlled (Spracklen et al., 2011; Kanakidou et al., 2000; Carlton et al., 2010).

The SOA formation and processing pathways in the atmosphere are remarkably complex. To represent these in ESMs, a trade-off must be made between detail and computational cost (Tsigaridis et al., 2014a). In reality, BVOCs consist of a myriad of compounds with different properties. However, in ESMs these are often reduced to be represented by 2-3 tracers, usually iso-

prene, monoterpenes (MTs) and sesquiterpenes which constitute the main contributors to aerosol formation and are estimated to constitute around 50%, 15% and 3% respectively of the total BVOC emissions (Guenther et al., 2012). The oxidation products of BVOCs, while in reality a large variety of compounds produced through a series of reactions (Glasius and Goldstein, 2016; Shrivastava et al., 2017), are lumped into a few tracers which can condense onto existing aerosols or contribute to NPF and early growth (Tsigaridis et al., 2014a). Not all oxidation products have low enough volatility to be relevant for aerosol formation. Therefore, the percentage of low volatility products formed during the oxidation is described by yields for each oxidation reaction (e.g. Tsigaridis et al., 2014a; Jokinen et al., 2015; Makkonen et al., 2014). Some models also use volatility basis sets or similar approaches to account for changes in volatility during the oxidation (Donahue et al., 2006, 2011; Yu, 2011).

All three models included in this study use two tracers representing the oxidation products from the BVOCs. One tracer represents the highly oxidized BVOCs which can take part in NPF and the early growth of the newly formed particles. This tracer will be denoted ELVOCs (Extremely Low-Volatile Organic Compounds) here. The other tracer represents the oxidation products with somewhat higher volatility that can condense onto larger aerosols, and will be denoted by L/SVOCs (Low/Semi-Volatile Organic Compounds). The VOCs are however not actually volatile in these models since the parameterizations only allow irreversible condensation of the organics.

As mentioned, evidence suggests that low-volatility organics contribute at the earliest stages of NPF (Tröstl et al., 2016; Riccobono et al., 2014; Ehn et al., 2014; Kirkby et al., 2016; Riipinen et al., 2011, 2012; Zhang et al., 2012b) and this is increasingly considered in global models. The formation / nucleation rate of new particles is typically parameterized with one parameterization of binary nucleation of sulfuric acid (H_2SO_4) and water (H_2O) vapours for the entire atmosphere. However, since these nucleation parameterizations underestimate NPF in the boundary layer (BL) (Spracklen et al., 2006), an additional parameterization involving sulphuric acid and organics that better capture the NPF in the BL is often added to the ESMs. These parameterizations are not always limited to the BL but in this manuscript we will refer to them as BL nucleation since they were introduced into the models to address the underestimation of NPF there.

There are large uncertainties in several of the processes representing SOA formation in ESMs. BVOC emissions are poorly constrained both locally and globally (Heald and Spracklen, 2015) and future changes in emissions are highly uncertain, both because of scenario uncertainty and because vegetation response is uncertain (Hantson et al., 2017). In addition, the formation of low-volatility oxidation products depends on a number of variables, including oxidation capacity, NO_x concentrations (Shrivastava et al., 2017), specific BVOC species etc., which results in large uncertainties in the yields (Jokinen et al., 2015). The representation of SOA in global models is currently under rapid development (Tsigaridis et al., 2014a; Makkonen et al., 2014; Gordon et al., 2016, 2017; Makkonen et al., 2012; Dunne et al., 2016). It is important to understand the dynamics introduced by these parameterizations and how they interact with the other parts of the models – in particular related to the direct and indirect aerosol effect, which have strong impacts on climate.

In this study we investigate the impact of choices in emissions of SOA precursors and yields of BVOC oxidation products on the climatic effects of SOA through a series of sensitivity experiments with three ESMs. The models have comparable treatments of SOA formation but have different aerosol schemes and different treatment of gas-phase chemistry. The comparison of

the simulations for the different models and experiments thus gives us the possibility to investigate the sensitivities to common parameters. We investigate how the direct and indirect aerosol effects are impacted by the changes in yields and emissions and from this, gain insight into how significant these parameters are for the radiative effects in the models. The goal is to better understand the processes controlling sensitivities in common setups of SOA parameterizations in ESMs currently. We do not conclude on whether these processes are treated correctly, but rather if it is important that they are.

2 Method

2.1 Experimental Setup

A set of sensitivity experiments were designed to investigate how changes to BVOC and SOA representations in the models affect clouds and radiation balance. Care was taken to design experiments that could be run with all three models. The 5 sensitivity experiments are:

- **Yield higher** - The EL/L/SVOC yields for the BVOC oxidation reactions (Table 2) are increased by 50 %.
- **Yield lower** - The EL/L/SVOC yields for the BVOC oxidation reactions are decreased by 50 %.
- **No ELVOCs** - The formation of ELVOCs is removed from the models. The total BVOC oxidation yields are kept constant but all BVOC oxidation reactions produce L/SVOCs.
- **No isoprene** - the isoprene emissions in the models are turned off.
- **No MTs** - the MT emissions in the model are turned off.

For comparison purposes, a control simulation (CTRL) was run with the models. The *Yield higher* and *Yield lower* simulations directly increase or decrease the produced SOA mass, while the changes are more complex for the other 3 experiments. The *No ELVOCs* scenario strongly decreases the NPF in the BL, and increases the mass of L/SVOCs which can only condense onto existing particles. With the *No isoprene* and *No MTs* cases, the importance of the two classes of BVOCs for modelled SOA mass and particle size distributions is investigated. Whereas isoprene is, on a global scale, emitted in larger amounts than MTs, its' oxidation reactions have smaller yields for SOA precursors than MTs. In addition, the modelled isoprene oxidation produces very little (EC-Earth, ECHAM) or no (NorESM) ELVOCs. Therefore, with these two experiments both the amount of modelled SOA and the fraction of oxidation products participating in NPF are changed.

In order to have similar meteorological conditions in the three models, all simulations were nudged (Kooperman et al., 2012) to ERA-Interim (Dee et al., 2011) data for the years 2000 - 2005. Although this method may not capture all changes in the cloud radiative effect (CRE) since dynamical feedbacks are limited by the constrained meteorology (Lohmann and Hoose, 2009; Lin et al., 2016), previous studies with CAM5.3-Oslo found the effective radiative from aerosol-cloud interactions (ERFaci) and ERFaci changes carried out with nudged configurations to be in the uncertainty range of that carried out with a free running version of the model (Kirkevåg et al., 2018; Karset et al., 2018). The first year of the simulations has been discarded as a

spin-up and the last 5 years have been used for the analysis.

The radiative effects from aerosols and clouds in this study are calculated using the methods described by Ghan (2013). The direct radiative effect (DRE) is calculated by taking the difference between the top of the atmosphere radiative flux and the radiative flux excluding scattering and absorption by aerosols (F_{clean}). The CRE is similarly calculated as the difference between F_{clean} and the radiation flux without the scattering and absorption by the clouds or aerosols ($F_{clean,clear}$).

2.2 Model similarities and dissimilarities

A more detailed description of each of the models will follow after this section. However, here we would like to highlight some of the key similarities and dissimilarities between the models (summarized in Table 1). The ESM model components are different between the three ESMs. The Norwegian Earth System Model (NorESM) and ECHAM have an atmospheric model which contains an aerosol module while EC-Earth consist of a chemistry transport model coupled to an atmospheric general circulation model. Therefore, EC-Earth has a more advanced treatment of gas-phase chemistry, including interactive oxidant fields, while the other two models have prescribed oxidant fields. The aerosol modules also differ between the models. NorESM has OsloAero (Kirkevåg et al., 2018) while EC-Earth and ECHAM both use M7 (Vignati et al., 2004), but different versions. As described in the Introduction, the treatment of the oxidation products is similar between the models where all three models have one ELVOCs and one L/SVOC tracer. However, the BVOC oxidation differs between the models in terms of yield, number of oxidation reactions from BVOC to ELVOCs/L/SVOCs and which reactions produce which oxidation products, as can be seen in Table 2. Moreover, all three ESMs use the Model of Emissions of Gases and Aerosols from Nature (MEGAN) ~~(Guenther et al., 2012) but forced with different underlying vegetation and meteorology, thus still generating different emissions in the different models~~ version 2.1 (Guenther et al., 2012). However, in NorESM, MEGAN is run interactively while the other two models use emissions produced in offline simulations with MEGAN.

2.3 NorESM

NorESM (Bentsen et al., 2013; Kirkevåg et al., 2013; Iversen et al., 2013) is an ESM based on the Community Earth System Model (CESM) (Neale et al., 2012). The aerosol scheme in the atmospheric community model (CAM) version 5.3 has been replaced by the aerosol scheme OsloAero (Kirkevåg et al., 2018). In this investigation, CAM5.3-Oslo (CAM with OsloAero) is coupled to the community land model (CLM) version 4.5 (Oleson et al., 2013) run with satellite phenology (SP) vegetation. NorESM is run with prescribed sea surface temperature (SST) and sea ice concentrations at 1.9 x 2.5° resolution. The horizontal winds and surface pressure are nudged to ERA-interim data with a relaxation time of 6 hours.

OsloAero is described as a production tagged aerosol model which consists of 12 lognormally shaped background modes. The shape and size of these modes can be modified by coagulation and condensation. The modes are made up of background tracers which determine the number concentration and process tracers which change the shape of aerosol size distribution. The mass of the tracers is tracked and the size distributions and optical properties are calculated using a look-up table approach (Kirkevåg et al., 2018).

NPF was recently added to OsloAero (Makkonen et al., 2014) and is now included as two background tracers, one for sulphate

(SO_4) and one for SOA, forming one mode (Kirkevåg et al., 2018). Two types of NPF are included in OsloAero; (1) Binary homogeneous sulphuric acid-water nucleation according to Vehkamäki et al. (2002) and, (2) an activation type nucleation, in the BL, with a nucleation rate calculated from Eq. 18 in Paasonen et al. (2010). This nucleation rate is calculated from the concentrations of H_2SO_4 and ELVOCs available for nucleation. The nucleation rates are calculated for particles with a diameter of 2 nm but the diameter of the nucleation tracers in OsloAero is 23.6 nm. The survival of these newly formed particles from nucleation to 23.6 nm diameter is parameterized dependent on coagulation sink and condensation growth rate in accordance with Lehtinen et al. (2007). In this study, contrary to Kirkevåg et al. (2018), we include all pre-existing particles in the calculation of coagulation sink. This modification was introduced into the model in order to have a more realistic survival rate of the particles between 2 and 23.5 nm.

The BVOC emissions used in the simulations are calculated interactively by MEGAN version 2.1 (Guenther et al., 2012) which is included in CLM. MEGAN thus uses the vegetation from CLM. The BVOC emissions depend on factors such as temperature, radiation, leaf area index and soil moisture. The model is run with half an hour time step and the coupling between CLM and CAM-Oslo is done at every time step providing an interactive diurnal variation in the emissions. The BVOC emissions include isoprene and 7 compounds which are lumped together as MTs in CAM-Oslo.

In CAM-Oslo, the emitted BVOCs are transformed into SOA through chemical reactions with ozone, ~~hydroxide~~ hydroxyl (OH) and nitrate radical (NO_3). When MTs reacts with O_3, ELVOCs are formed, while the other five reactions yield only L/SVOCs. The reactions and their yields are given in Table 2. 50 % of the formed ELVOCs is available for nucleation and the rest of the ELVOCs and the L/SVOCs condense onto pre-existing aerosol particles (Makkonen et al., 2014). The molar mass of both the ELVOCs and L/SVOCs are 168 g mol^{-1}. The oxidants are prescribed monthly fields originating from a run with the full chemistry model CAM-chem (Lamarque et al., 2012).

CAM5.3-Oslo uses the cloud bulk microphysics scheme MG1.5 (Morrison and Gettelman, 2008; Gettelman and Morrison, 2015) with aerosol activation by Abdul-Razzak and Ghan (2000) for the stratiform clouds. Mass and number of cloud water and ice are treated prognostically while the precipitation is diagnostic. The model also includes a shallow convection scheme (Park and Bretherton, 2009) and a deep convection scheme (Zhang and McFarlane, 1995).

2.4 EC-Earth

The Earth system model EC-Earth (Hazeleger et al., 2012; van Noije et al., 2014) includes an atmospheric general circulation model (GCM) based on cycle 36r4 of the Integrated Forecasting System (IFS) of the European Centre for Medium-Range Weather Forecasts (ECMWF). This is coupled to the atmospheric chemistry and transport model TM5 (Tracer Model 5, van Noije et al., 2014; Williams et al., 2017). For the present study, the EC-Earth release v3.2.3 in atmosphere-only mode (i.e., IFS + TM5) was used. TM5 treats the emission, transport, microphysical and chemical conversions, and deposition of atmospheric gases and aerosols. The latter are described with the size-resolved modal microphysics scheme M7 (Vignati et al., 2004). It uses seven log-normal size distributions (modes) of which four are soluble (nucleation, Aitken, accumulation, coarse) and three insoluble (Aitken, accumulation, coarse). The nucleation, Aitken, accumulation, and coarse mode represent particles with dry diameters smaller than 10 nm, 10-100 nm, 100 nm - 1 μm, and larger than 1 μm, respectively. The considered aerosol species are

sulphate, black carbon, organic matter (primary and secondary), mineral dust, and sea salt. M7 tracks the number concentration in each mode and the mass of each species in each mode. The mode shape is constant whereas median diameter, number of particles of each mode and their chemical composition can evolve freely. After growth by condensation and coagulation, the largest particles of each mode are shifted to the next larger mode. Particles in the insoluble modes that reach sufficient soluble coating are shifted to the respective soluble modes.

In addition, TM5 simulates the total particulate mass of nitrate, ammonium, and methane sulphuric acid. When calculating optical properties these components as well as the associated water uptake are assumed to be in the soluble accumulation mode. The gas-phase chemistry is described by a modified version of the Carbon Bond 05 (CB05) mechanism (Williams et al., 2017) using the photolysis scheme from Williams et al. (2012). SOA is produced from MTs and isoprene with the yields as presented in Table 2. Assumed molar masses for the two SOA species, ELVOCs and L/SVOCs, are 248 g mol^{-1} and 232 g mol^{-1}, respectively. Produced ELVOCs condense to soluble nucleation, Aitken, accumulation, and coarse mode as well as to insoluble Aitken mode according to the respective condensation sink (depending on surface area). L/SVOCs condense to soluble Aitken, accumulation, and coarse mode as well as insoluble Aitken mode according to the actual mode mass.

NPF is treated following Vehkamäki et al. (2002). In addition, NPF from H_2SO_4 and ELVOCs is calculated using the semi-empirical method by Riccobono et al. (2014) (see Table 1). The size of freshly nucleated sulphuric-acid-ELVOC-clusters is assumed to be ~~2~~ 1.7 nm. The early growth to 5 nm diameter is calculated following Kerminen and Kulmala (2002). The resulting number of these 5 nm-particles are finally added to the nucleation mode.

The emission of the SOA precursors isoprene and MTs are calculated using MEGAN-MACC (Sindelarova et al., 2014) for the year 2000 and depend on the underlying vegetation information. The BVOC emissions are prescribed monthly fields and with an applied diurnal variation. There is also small fraction of MTs and isoprene emitted from biomass burning, which will participate in production of SOA.

For the present study, IFS is applied at a spectral truncation of T255 (corresponding to 0.7°) grid with 91 vertical levels. Emissions for TM5 are applied on a $0.5° \times 0.5°$ grid whereas following processes and transport are calculated on $3° \times 2°$. The horizontal winds (via divergence and vorticity) and surface pressure were nudged against ERA interim with a relaxation time of 8.25 hours. The cloud droplet number concentration of stratiform clouds is calculated using Abdul-Razzak and Ghan (2000), and both determines the effective radius of the cloud droplets and influences the lifetime of the clouds via its effect on the autoconversion of cloud liquid water to rain.

2.5 ECHAM

ECHAM5-HAM (Stier et al., 2005) is an aerosol-climate model originally developed at the Max Planck Institute for Meteorology, Hamburg. The Hamburg Aerosol Module (HAM) also employs the M7 aerosol microphysics module. The ECHAM-HAM simulations were performed in T63 spectral resolution with 31 hybrid-sigma vertical levels. The spectral atmospheric variables are nudged with standard ECHAM relaxation timescales: 6 h for vorticity, 24 h for pressure and temperature, and 48 h for divergence (Lohmann and Hoose, 2009).

We apply a modified version of ECHAM5.5-HAM2 (Zhang et al., 2012a), which uses an improved numerical scheme (Kokkola

et al., 2009) to compute the formation of sulphuric acid by oxidation of SO_2, and its removal by nucleation and condensation on pre-existing particles. We consider SOA formation from the biogenic precursors isoprene and MTs. The SOA formation mechanism (Jokinen et al., 2015) includes both kinetic condensation to Fuchs-corrected surface area (condensation sink)~~and partitioning~~. Moreover, the relative partitioning to the Aitken/accumulation/coarse mode is done according to pre-existing organic mass in the respective modes. The model considers three BVOC tracers: isoprene, endocyclic and other MTs. The BVOC emissions in ECHAM simulations were pre-computed monthly averages (Jokinen et al., 2015). The MEGAN2.1 (Guenther et al., 2012) was driven with input drivers described in Sindelarova et al. (2014), combining MERRA meteorological fields and MACC landcover data. However, the BVOC emission inventories did not separate endocyclic and other MTs, hence their respective emissions were considered equal fractions. The reaction rates of SOA precursors with O_3, OH and NO_3 are described in Jokinen et al. (2015).

The ELVOC yields are based on extensive laboratory experiments (Jokinen et al., 2015), while the total (ELVOC+L/SVOC) yield is set to 15% for MTs and 5% for isoprene. ELVOCs provide early growth for nucleation mode particles, as they are distributed to the particle phase according to condensation sink. The low- and semi-volatile products are distributed to particle phase according to particle-phase organic mass, as in Jokinen et al. (2015). Hence, after oxidation, no SOA products remain in the gas-phase, but immediate condensation to aerosol-phase is assumed. Simulations include organic vapours in the nucleation process according to Eq. 18 in Paasonen et al. (2010). The growth from nucleation to 3 nm is calculated according to Kerminen and Kulmala (2002) assuming growth by ELVOCs and sulfuric acid.

3 Results and discussions

We will start the results section by investigating the inter-model differences in the CTRL simulation among the three models. It is necessary to be aware of the differences between models before investigating at the changes that the sensitivity simulations induce.

3.1 CTRL

3.1.1 BVOC emissions and concentrations

The three ESMs all use the same emission model (MEGAN) but the emissions of MTs and isoprene still vary between the models because of choices in land cover data and meteorology. For isoprene, NorESM has the lowest emissions rates of about 435 Tg yr^{-1} while EC-Earth and ECHAM are somewhat higher with 572 and 526 Tg yr^{-1} , see Fig. 1g. The spatial distribution in the emissions also varies between the models. In NorESM, the isoprene emissions are highest in the Amazon region with somewhat smaller sources in Africa and the tropical islands of Indonesia (Fig. 1a). EC-Earth has the highest emission rates out of all models but with the Amazonian maximum located further south than in NorESM (Fig. 1c). ECHAM has similar emission patterns to EC-Earth but with somewhat weaker emissions, see Fig. 1e.

For MTs, NorESM has the highest global emissions (118 Tg yr^{-1}) followed by EC-Earth (96 Tg yr^{-1}) and then ECHAM (77 Tg yr^{-1}) as can be seen in Fig. 1h. The largest differences in the emissions are in the tropics, in particular in the Amazonian region, where NorESM has up to twice as high annual emissions. The cause of the difference in emissions is related to the implementation of MEGAN used in the models. In NorESM, MEGAN is interactive and uses the vegetation from CLM as well as atmospheric conditions and radiation in the calculation of the BVOC emissions. EC-Earth and ECHAM on the other hand use prescribed BVOC emissions from MEGAN-MACC with a yearly as well as diurnal variation included (Sindelarova et al., 2014). The emissions from these two models are not the same because different meteorology was used in the generation of the emissions fields.

The column burdens of the BVOCs also differ between the models (not shown). The global mean column burden of isoprene is approximately three times higher in EC-Earth (1.0 kg m^{-2}) than in the other two models. This is in part because of significantly higher column burdens over the strong emission regions in South America and Africa, which are due to the interactive oxidant fields in EC-Earth. When interactive oxidant fields are used the oxidants can be depleted and as a result the lifetime of BVOCs is increased. This does not occur in the other two models that have prescribed oxidation fields. The MT column burdens are more similar between the models.

3.1.2 SOA formation and aerosol size distributions

There is a large range in the amount of SOA formed in the different models. In spite of having the lowest BVOC emissions (due to lower isoprene emissions), NorESM has the largest average annual production (85 Tg yr^{-1}) while ECHAM and EC-Earth have very similar and somewhat lower SOA production (52 Tg yr^{-1}), see Fig. 2a. The higher emissions in NorESM is likely a result of the higher MT emissions (which have the highest yields), in combination with higher yields for isoprene than EC-Earth. Also the assumed molar mass of the BVOC oxidation products will affect how much SOA mass is formed. The produced SOA mass in the models are in the range of the values found in Tsigaridis et al. (2014b) but are higher than the median of the models included in that study.

In this paper we have averaged the size distribution and number concentration data globally over the model levels with pressures higher than 850 hPa, i.e the bottom part of the atmosphere. This choice was made since this part of the atmosphere contains most of the aerosol mass which is relevant for both the direct and indirect aerosol effects. Moreover, clouds in the ESMs use aerosol activation at the bottom of the clouds and thus, the aerosols at these levels are most important also for the indirect aerosol effects. The aerosol size distributions (for all particles) show large differences between the models even though ECHAM and EC-Earth both use the modal aerosol model M7, see Fig. 3. The most noticeable difference between the number size distribution of the models is that NorESM, which uses the aerosol model OsloAero, has no explicit nucleation mode. In NorESM, particles from NPF are added directly into SO_4/SOA nucleation mode which is in the Aitken-accumulation size range after growth through condensation. ECHAM's size distribution is dominated by a large nucleation mode which contains almost two orders of magnitude more particles than the nucleation mode in EC-Earth. Moreover, EC-Earth also has fewer particles than the other models in the largest particle sizes (diameters > 250 nm). Of the three models, ECHAM has the most particles at large sizes (diameters >300 nm) as well as highest surface and volume of particles (Fig. 3 b and c). Total aerosol number concentrations

(Fig. 4) reveal that EC-Earth has the lowest aerosol number concentrations out of all models and ECHAM has the highest. This is still the case when comparing the number concentrations without the nucleation mode. Moreover, ECHAM has substantially higher aerosol number concentrations over the remote oceans (Fig. S1) compared to the other two models. There are likely many different explanations to why the size distributions and aerosol number concentrations are different in the models. Some plausible explanations include differences in wet deposition, nucleation rates and how the emissions in general are partitioned into the aerosol modes.

3.1.3 AOD and direct aerosol effects

The global average aerosol optical depth (AOD) is highest in NorESM, 0.19, (Fig. 2b) due to significantly higher AOD values over desert regions, in particular the Sahara (Fig. S1). This is associated with high dust emissions from the dessert. ECHAM has the second highest global AOD values (0.16) and has somewhat higher AOD values over the ocean than the other two models. The direct aerosol effects (Fig. 2c) in the models resemble the results from the AOD. EC-Earth has lower globally averaged direct radiative effect (DRE_{Ghan}) than the other two models. This is a result of the low aerosol number concentrations, in particular at larger, radiation relevant sizes. This can also be seen in the AOD from EC-Earth. ECHAM has slightly stronger global average DRE_{Ghan} than NorESM even though NorESM has a higher average AOD. The reason for this is that many of the regions with large AOD in NorESM have very bright surfaces (e.g. deserts) and therefore result in a lower DRE_{Ghan} (Fig. S1).

3.1.4 Cloud properties and indirect aerosol effect

The cloud properties in CTRL simulation are quite different in the models. EC-Earth has the lowest cloud droplet number concentrations (Fig S2) which is related to the low number concentrations of aerosol particles in this model. ECHAM on the other hand has the highest number of cloud condensation nuclei (CCN) and also the highest cloud droplet number concentrations (CDNC). NorESM has larger droplet sizes than the other two models and the droplet size patterns are very different in the different models. Nevertheless, the total grid box cloud water path (CWP) is fairly similar between the three models, but slightly higher in EC-Earth (Fig. 2d). The total cloud fractions (CF) in the models are also fairly similar with global average values between 0.61 and 0.67, see Fig. 2e. The cloud radiative effect (CRE_{Ghan}), is stronger in NorESM (-31 W m^{-2}) compared to EC-Earth (-23 W m^{-2}) and ECHAM (-26 W m^{-2}), see Fig. 2f. Note that these are development version of NorESM and EC-Earth which has not been tuned. The patterns of the CF and CRE_{Ghan}can be seen in Fig. S3.

3.2 Yield higher and Yield lower

The results from the sensitivity simulations will now be presented and discussed in three different sections. The sensitivity experiments are grouped according to the similarity in the results. In the first section, the *Yield higher* and *Yield lower* experiments are discussed.

3.2.1 Direct aerosol effects

First, the results regarding the changes in aerosol scattering and how these affect climate forcing are presented. In the *Yield higher* simulation the DRE_{Ghan} becomes stronger, i.e. more negative, and the opposite is true for the *Yield lower* simulation, for all three models (Fig. 5). These changes reflect the changes in SOA formation (Fig. 6) as more SOA leads to a stronger DRE_{Ghan}. Since NorESM has the largest SOA production it also experiences the largest SOA production change in these simulations, approximately $\pm$ 38 Tg per year. The changes in the other two models are in the order of 25 Tg per year. Interestingly, an increase / decrease in the SOA precursor yields by 50 % results in an increase / decrease in SOA production by 50 % only in EC-Earth. In NorESM, the SOA production change is somewhat less than 50 % in both simulations. The explanation for this is that SOA is also produced from dimethyl sulphide (DMS) emissions from the ocean in NorESM (Kirkevåg et al., 2018), and these yields are not changed in the sensitivity simulations. For ECHAM, the effect is somewhat larger in the *Yield higher* simulation (+52 %) and smaller in the *Yield lower* simulation (-45 %).

The degree to which a SOA increase leads to an strengthening in the DRE_{Ghan} varies between the models. NorESM has the largest absolute increase / decrease in SOA formation in these two simulations but it is EC-Earth that experiences the largest change in the DRE_{Ghan} with changes of $\pm$ 0.15 Wm^{-2}. For reference, this number is roughly half of the radiative forcing due to aerosol–radiation interactions (RFari) best estimate in the Fifth Assessment Report by the IPCC (2013). ECHAM has the smallest changes in DRE_{Ghan} with values of approximately $\pm$0.03 even though this model has similar changes in SOA production changes to EC-Earth. The cause of the different responses in the different models is, at least partly, related to where in the aerosol size distribution the additional / removed SOA is located. For all three models in the *Yield higher* simulation, the globally averaged particle number concentrations increase at sizes relevant for scattering of solar radiation ($\text{N}_{d>100}$, number concentration of particles above 100 nm) (see Fig. 4). In ECHAM however, this increase is quite small, see Fig. 4f. The changes in particle number concentration in NorESM are quite large but are mainly located close to the BVOC sources (not show). EC-Earth instead experiences these changes in the particle number concentration further downwind of the sources. This results in a more widespread change in DRE_{Ghan} in EC-Earth compared to the other two models (see Fig. S4) and thus a significantly higher global average DRE_{Ghan}. Similar but opposite changes are seen in the *Yield lower* simulation.

3.2.2 Indirect aerosol effects

The response of the indirect aerosol effects in the *Yield higher* and *Yield lower* sensitivity test differ more than the direct effects. The CRE_{Ghan} in NorESM is strengthened (i.e. more negative) with increasing SOA production and vice versa, see Fig. 7. The changes in CRE_{Ghan} are -0.27 W m^{-2} (*Yield higher*) and 0.35 W m^{-2} (*Yield lower*) indicating that these sensitivity simulation induce changes in the forcing of relevant magnitude. The globally averaged changes in EC-Earth have the same sign as those for NorESM but are lower (-0.11 and +0.076 W m^{-2}), and for ECHAM the changes are very small and not statistically significant. Also for the indirect effects, changes in the size distributions can be used to explain the changes in CRE_{Ghan}. While hygroscopisity might play a role, the effect is small in the activation scheme shared by the models (Abdul-Razzak and Ghan, 2000).

For NorESM, the higher (lower) SOA production in the *Yield higher* (*Yield lower*) simulation results in a shift in the size distribution to larger (smaller) sizes, see Fig. 4. For the *Yield higher* simulation, this results in higher CCN concentrations, higher CDNC, smaller cloud droplet effective radius (r_e) and ~~smaller~~ larger CWP (Fig S4 - S7). The opposite change in these variables is seen in the *Yield lower* simulation. The main relative changes in cloud variables in NorESM are located over and downwind of the large BVOC emission sources in the Tropics. Increased number of CCN generally means higher CDNC, lower r_e and higher CWP in all three models. For some regions, the CF decreases as CCN increases. The results regarding the changes in cloud parameters are shown in Fig. S5 - S8 for the *Yield higher* and *Yield lower* simulations. Since the cloud response to the CCN changes are similar in all the models and simulations, we will mainly discuss CCN and CRE_{Ghan} changes for the other simulations.

The essentially non-existing effects on the CRE_{Ghan} in ECHAM can also be explained using the size distribution. ECHAM experiences the smallest changes in particle number concentrations for particles with diameters > 100 nm, see Fig. 4f. However, for the smallest size ranges (N_{1-60}) ECHAM has the largest changes in the concentration of particles. Not surprisingly, the changes in number of these small particles do not affect the cloud formation in ECHAM, probably because they are too small to act as CCN when there is an abundance of particles at larger sizes (accumulation mode). Another interesting feature of ECHAM is that the changes in the size distribution are not mirrored in *Yield higher* and *Yield lower* simulation, which suggest non-linear dynamics caused by competition between NPF and condensation sink.

The rather small global changes in CRE_{Ghan} for EC-Earth are somewhat surprising since this model had the strongest response for the DRE_{Ghan}. However, investigating the maps of the changes in the CRE_{Ghan} for EC-Earth in Fig. 8 c-d, one can see that the low global responses are caused by a pattern of opposite changes with magnitudes up to 4 Wm^{-2}. In the *Yield higher* simulation, there is a strengthening of the CRE_{Ghan} close to large BVOC emission regions in the Tropics, while over the remote oceans there is a weakening instead. The mirrored response is seen in the *Yield lower* simulation. Since the SOA production increases (decreases) globally in the *Yield higher* (*Yield lower*) simulation, the opposing patterns of CRE_{Ghan} are not directly related to changes of SOA production. Instead, the changes are related to different effects on the size distribution close to and far away from the BVOC sources as can be seen in Fig. 9 (the areas are shown in Fig S21). For the *Yield higher* simulation, close to the sources, the increase in SOA production results in more accumulation mode particles ($N_{100-500}$), which leads to higher CCN concentrations and a stronger CRE_{Ghan}. Over the remote regions there is also an increase in accumulation mode particles, but this is accompanied by a larger decrease in particle concentrations in the Aitken mode (N_{20} - N_{60}). Since the aerosol concentrations are low in EC-Earth, in particular in these remote regions, the particles in the Aitken mode can also be activated as CCN because reduced competition effects gives higher maximum super saturation during cloud droplet activation. As a result, the CCN concentrations in these remote regions decrease when the SOA formation increases. This leads to a weakening of the CRE_{Ghan} (positive values). The changes in the *Yield lower* mirror those in the *Yield higher* simulation.

3.3 No ELVOCs

In this second section of results from the sensitivity simulations the results from the *No ELVOCs* simulation are presented. This simulation is different from the other simulations since only the type of SOA precursors is changed and not the amount of precursors.

3.3.1 Direct aerosol effects

In terms of the direct effects, the global changes are small in all three models. For NorESM there is a small but statistically significant strengthening of the DRE_{Ghan}, but the other two models do not display significant changes (see Fig. 5). The change in NorESM can be explained by changes in aerosol number concentrations over and downwind of the Amazon. Since there is no ELVOCs contributing to nucleation in this simulation, the NPF is reduced, and with this the number concentration of smaller particles. This decrease is particularly strong over the Amazon since the MT emissions are very high here (see Fig 1b) and ELVOCs can only be produced from MTs in NorESM. The strong decrease in small particles and increased vapours available for condensation (L/SVOCs) in this region means that more particles can grow to sizes where they act as efficient scatterers of solar radiation. This effect over the Amazon in NorESM is big enough to affect the global DRE_{Ghan}.

NorESM produces a large number of particles close to the BVOC emissions sources and, since the model does not contain a nucleation mode these particles are introduced into the Aitken mode. The nucleated particles thus reach larger sizes closer to the sources than in other two models where the particles are introduced into a nucleation mode and shifted to the Aitken mode at a later time step, while they are transported. This could be part of the explanation of why the BVOC effects in NorESM, in general, are located closer to the sources than in EC-Earth. Moreover, in comparison to NorESM, EC-Earth has lower oxidant concentrations close to the large BVOC sources (not shown), which limits the SOA production in these regions and increases the amount of BVOC transported away from the sources. Hence, the overall effect is more widespread than in NorESM.

3.3.2 Indirect aerosol effects

For the indirect aerosol effects, EC-Earth is the only model that has significant changes for this simulation. The CRE_{Ghan} is weakened (less negative) by 0.44 Wm^{-2} as can be seen in Fig. 7. This strong change in the CRE_{Ghan} is caused by a more or less strong worldwide decrease in the aerosol number concentration at almost all sizes (except particles above 500 nm). This results in a reduction of CCN which leads to a weakened CRE_{Ghan}. This strong decrease in CCN in EC-Earth occurs since the nucleation rates involving ELVOCs are calculated from a product of the H_2SO_4 and ELVOC concentrations (see Table 1). Thus, the removal of ELVOCs in this simulation removes all the BL NPF in EC-Earth. The other two models instead calculate the nucleation rates as the sum of H_2SO_4 and ELVOC concentrations and thus retains BL NPF from H_2SO_4. This results in quite different spatial patterns of the reduction in total aerosol number concentrations in the different models. For NorESM and ECHAM, the reductions occur close to the BVOC sources. For EC-Earth on the other hand, the reductions are largest over regions that have large anthropogenic SO_2 emissions such as Europe, North America and Australia (not shown). This widespread reduction in CCN in combination with EC-Earth having low aerosol concentrations (which makes the clouds

more sensitive to aerosol perturbations (Spracklen and Rap, 2013)) results in a significant weakening of the CRE_{Ghan} in this simulation.

ECHAM has no significant change in the CRE_{Ghan} when the ELVOCs are removed. As for the first two experiments, the changes in the particle concentrations in the accumulation mode are small (Fig. 4). ECHAM, unlike the other models, experience an increase in nucleation mode particles in this simulation. This is somewhat unexpected since removal of ELVOCs is expected to result in a decrease in NPF. This simulation however shows that the nucleation rate parameterization in ECHAM is not very sensitive to ELVOC concentrations. Nevertheless, the growth of the newly formed particles is highly dependent on the ELVOC concentrations and since the particles do not grow to larger sizes, more particles remain in the nucleation mode. This results in increasing the concentration in the nucleation mode and decreasing number concentrations at larger sizes.

3.4 No isoprene and No MTs

In this last result section the *No isoprene* and *No MTs* simulations will be shown and discussed.

3.4.1 Direct aerosol effects

The DRE_{Ghan} is reduced (less negative) in all models in both these simulations since the SOA formation goes down when the BVOC emissions are reduced. The strongest effects on the DRE_{Ghan} is seen in EC-Earth with approximately 0.15 W m^{-2} changes for the *No isoprene* and *No MTs* simulations (Fig. 5). The reductions in DRE_{Ghan} for NorESM are about twice as large as those for ECHAM for the *No MTs* simulation. Moreover, both NorESM and ECHAM have almost an order of magnitude smaller decreases than in EC-Earth. In NorESM and ECHAM the changes in DRE_{Ghan} are located fairly close to the sources while in EC-Earth they have a larger geographical spread (Fig. S15). This is the main cause for the large changes in the global DRE_{Ghan} in EC-Earth. The decrease in DRE_{Ghan} is explained by a reduction in the concentration of particles relevant for scattering (diameters above 100 nm).

The difference in SOA production between these cases reflects the proportion of SOA originating from isoprene and MTs respectively. NorESM and ECHAM have the largest reductions in the *No isoprene* case, indicating that isoprene is the dominant SOA precursor, while EC-Earth has the largest reduction in the *No MTs* simulation, indicating MTs are the dominant precursors. The difference in dominating precursors in the different models is mainly a result of different yields. The EC-Earth isoprene yields are 1 % (ELVOCs + L/SVOCs), 15 times lower than for MTs, while in NorESM and ECHAM, the isoprene yield is 5 %, 3 times smaller than for MTs.

In the *No isoprene* simulation we also see an interesting feature connected to the interactive gas-phase chemistry in EC-Earth. Over large emission regions in the Tropics, the column burden of MTs decreases when we remove the isoprene emissions, see Fig 10. The decrease in the MT column burden is caused by a greater availability of OH when there is no isoprene present. The concentration of O_3 is reduced ~~, but~~ since the oxidation of of isoprene results in the production of O_3. However, the loss rate of MT to O_3 oxidation is less important ~~for the loss rate~~than OH, and thus the overall result is a reduction in column burden. This occurs only in EC-Earth due to the interactive chemistry in TM5. This does not increase the amount of SOA formed from MTs but it affects where this SOA is formed, causing formation of SOA to occur closer to the sources. Additionally it favours

the L/SVOCs over ELVOCs (see Table 2) because oxidation with OH will dominate more over reactions with O_3, and MT oxidation with O_3 have a higher ELVOC yield (5%) than with OH (1%).

3.4.2 Indirect aerosol effects

The *No isoprene* simulation displays the largest and also the most divergent results out of all simulations for the indirect aerosol effects. NorESM has a weakened CRE_{Ghan} by 0.53 W m^{-2} while EC-Earth has a strengthened CRE_{Ghan} by -0.82 W m^{-2}. These numbers show that there is a substantial impact on the CRE_{Ghan} from the isoprene emissions in NorESM and EC-Earth. The magnitude of these numbers are in the range of and larger than the best estimate of the IPCC (2013) ERFaci relative to 1750 of -0.55 W m^{-2}. ECHAM on the other hand experience a non-significant change in CRE_{Ghan} in, see Fig. 7. Interestingly, all three models show a somewhat similar change in the size distribution as can be seen in Fig. 4. Isoprene mainly produces L/SVOCs in the models and the removal of isoprene therefore leads to a shift in the particle size distribution towards smaller particles. For ECHAM, the aerosol concentration changes at CCN relevant sizes are very small and the clouds are virtually unaffected by this change. NorESM on the other hand, experiences a quite large decrease in accumulation mode particles which results in a decrease in CCN and weakening of the CRE_{Ghan}. EC-Earth also experience a decrease in particles above 100 nm. Moreover, the Aitken mode in EC-Earth has a large absolute increase. This is due to more NPF when the condensation and coagulation sink decreases (more on this in the next section). Since the aerosol number concentrations in EC-Earth are so low, even aerosol particles in the Aitken mode can be activated as CCN and the increase in Aitken mode particles leads to increased CCN concentrations. This results in a strengthening of the CRE_{Ghan}, in particular over the oceans (Fig S20). Thus, similar changes in the size distribution lead to vastly different responses in the three models depending on aerosol number concentrations and different size distribution dynamics.

For the *No MTs* simulation, EC-Earth and NorESM have a weakened CRE_{Ghan} while ECHAM experiences no significant change in the CRE_{Ghan}. The MT oxidation is the main source for ELVOCs in all 3 models (the only source in NorESM). It was therefore expected that turning off the emission of MTs would reduce the amount of small particles in the models. However, this behaviour is only seen in EC-Earth where the global mean particle number concentration decreases at all sizes globally (see Fig. 4). For NorESM, the number of small particles instead increases while the number of larger particles decreases (due to less condensational growth of the particles), indicating that the loss of L/SVOCs (condensation) from MTs is more important than the loss of ELVOCs (NPF) for the size in this model. In ECHAM the number of nucleation mode particles increases and the number of larger particles decreases, which reduces the sink for small nuclei. Similarly to the *No ELVOCs* simulation the reduction in ELVOCs leads to limited growth of the nucleation mode particles and therefore, an increase in this mode. However, the changes in ECHAM are again very small and do not affect the clouds. Both NorESM and EC-Earth experience a decrease in CCN and therefore a weakened CRE_{Ghan}. The global CRE_{Ghan} response in EC-Earth in this simulation is, as for the simulations with changed yields, a result of compensating opposite patterns of CRE_{Ghan} close to (weakening) and far away (strengthening) from the sources.

3.5 Further discussion and implications

The introduction of particles from NPF should in theory and in the models be dependent on the interplay between available vapours for nucleation, condensation losses of these vapours and loss of newly formed particles due to coagulation. Adequately parameterizing these processes is a challenge and the balance between them varies between the models, and also sometimes between regions in the same model. Regional variation is seen EC-Earth where the NPF response varies depending on the distance from the sources, even if both regions experience the same sign in SOA production change. Taking the *Yields lower* experiment as an example: Close to the sources, the decrease in VOCs lead to a reduction in both larger particles and NPF (Fig. 9). In remote regions on the other hand, the coagulation sink for newly formed particles is reduced because of a reduction in larger particles. This increases the probability of NPF particles surviving to larger sizes. Thus, even though the total aerosol mass is decreased, the mass is partitioned to smaller sizes and the total number concentration is increased. Finally, since EC-Earth generally has low particle number concentrations in these regions, even these smaller particles are activated to form cloud droplets and produce a negative CRE. A similar effect can be seen in the *No isoprene* case for EC-Earth where we also see a strong negative CRE_{Ghan} associated with an increase in number concentrations (in spite of a decrease in total mass), see Fig. 7 and 6.

The above example for EC-Earth raises a more general point: The relationship between SOA production and CCN and aerosols relevant for radiation is highly non-linear. If ELVOCs are important for NPF and early growth, then an increase in ELVOCs could lead to more particles formed, but also less condensate to grow the existing particles to climate relevant sizes (CCN, direct radiation effects). On the other hand, if H_2SO_4 is driving the NPF, SOA might be more important through changing the coagulation sink for NPF, and more SOA could lead to less NPF, and the effect on CCN will depend on the particles that are left. Thus, NPF does not necessarily lead to higher CCN concentrations.

Another factor of importance to NPF impact on the size distribution is the size at which new particles are added to the aerosol scheme. In EC-Earth and ECHAM, the particle growth and survival to 3 nm (ECHAM) and 5 nm (EC-Earth) are parameterized separately, and then the particles are added to the nucleation mode. The size at which these particles are added make a difference for the transferal of particles to the Aitken mode: in EC-Earth the added particles at 5 nm are already above the number median diameter of the mode and thus some of these will always be transferred to the Aitken mode. In ECHAM on the other hand, the addition of newly formed particles to the nucleation mode will decrease the number median diameter of the mode and can even decrease the number of particles that are transferred to Aitken mode. If NPF is continuously high, the particles can thus even be inhibited to grow to larger sizes. How much the radius of modes are allowed to change in combination with adding the particles at different sizes could be part of the explanation why EC-Earth and ECHAM show such different changes in aerosol size distributions even though both models use the M7 aerosol module. NorESM also has a separate parameterization for the growth and survival of the NPF particles up to a radius of 23 nm when the particles are added to the tracer for NPF. This growth occurs in one time step of the model (30 min). Hence, the particles grow very rapidly and reach Aitken mode sizes close to the sources.

This investigation shows that interactive oxidants can play an important role in determining, in particular, where the SOA

formation occurs. The reduction in MT column burden over tropical forests when isoprene is removed illustrate that using interactive oxidants, may limit the SOA formation in certain regions. This shifts the SOA formation further downstream from the sources which results in more widespread climatic effects from BVOCs. Moreover, the results from the *No isoprene* in the EC-Earth model show that there can be feedback mechanisms through interactive oxidants that affect SOA formation. In general, the removal of isoprene results in less formation of O_3 since it's production is linked to the oxidation of isoprene. The reduction in O_3 means there is less O_3 available for SOA formation which can lead to a further reduction in SOA production. Nevertheless, in the *No isoprene* simulation the removal of isoprene also leads to a higher availability of OH for the oxidation of monoterpenes, which then is oxidised closer to the sources. This results in an increase in SVOC formation from monoterpenes. In summary, changes in emissions can feed back to SOA formation both through effects on the oxidation capacity of the atmosphere and through changing the balance between the oxidants and thus the total SOA production due to different yields for different oxidants.

There are clearly large differences in the aerosol size distributions and how the changes in these sensitivity experiments affect the size distributions in the models. This is in spite of quite similar simplified treatments of SOA formation in the three models. Our findings show that the location of the SOA mass in the size distribution is critical for CCN concentrations, which agree with the results in Riipinen et al. (2011). The present study implies that further model development and evaluation is needed in terms of how new particle and SOA formation affect the size distribution. However, there are still large uncertainties on how these models should behave with regards to these processes (Glasius and Goldstein, 2016; Riipinen et al., 2011).

There are however also other uncertainties and limitations with regards to the SOA processes in these models. One such limitation in the models in this study is the assumption that L/SVOCs are condensing irreversibly on preexisting aerosol particles. More realistic parameterizations of this process, such as Volatility Bases Set parameterizations, are starting starting to make their way into global climate models (Tsigaridis and Kanakidou, 2018). However, the gain from introducing a number of additional tracers required in such parameterizations need to be balanced against the increased computational expense to become readily used in ESMs. Another limitation is the lack of anthropogenic SOA in the models, as currently, all anthropogenic emissions are treated as primary emissions. Anthropgenic impact on SOA formation trough gas-phase chemistry, e.g. NOx impact on yields, is also not included in these models at this point. Impacts from vegetation on the organic aerosol budget trough primary biological organic aerosols, are also missing in this study. The treatment of organic aerosol in ESMs is currently in rapid development. Model evaluation against observations is an important tool in this development work, though it is out of the scope of this manuscript.

Over the past years, more and more studies have investigated the BVOC climate impact from pre-industrial to present day (Heald and Geddes, 2016; Scott et al., 2017; Unger, 2014) and also into the future, including possible BVOC climate feedbacks (Sporre et al., 2019; Makkonen et al., 2012; Scott et al., 2018; Paasonen et al., 2013). The results regarding the BVOC impact on climate have a large spread among the different studies. This study indicates that at least parts of these differences could be related to varying sensitivity to BVOC and SOA changes in the models used in the different studies. The decrease in isoprene emissions since 1850 has been estimated to be approximately 15 % (Scott et al., 2017; Unger, 2014) and in this study, the removal of all isoprene emissions leads to a change in the total aerosol radiative effect by 0.62 W m^{-2} in NorESM

and -0.67 W m^{-2} in EC-Earth, a 1.29 W m^{-2} difference. Hence, assuming the changes in radiative effects are not too far from linear, the decrease in isoprene emissions since pre-industrial would introduce an uncertainty in the aerosol forcing of order of magnitude 0.19 W m^{-2} using these models. This sensitivity study reveals that NorESM, EC-Earth and ECHAM would produce very different results if used to investigate the climatic impacts of BVOCs.

4 Conclusions

The impact of BVOC emission and SOA formation on particle size distribution, cloud properties and radiative effects have been compared among three ESMs, NorESM, EC-Earth and ECHAM. In five different sensitivity studies, the effect of changed yields of BVOC oxidation, volatility of the oxidised BVOCs, contribution of precursor gases has been investigated.

We found that both the direct and indirect aerosol effects in the models are substantially affected by changes in SOA precursor yields and BVOC emissions. The DRE_{Ghan} is strengthened (by up to 0.15 Wm^{-2}) by more SOA and vice versa. Even though the changes in DRE_{Ghan} have the expected sign of the response to changes in SOA production in all three models and simulations, the sensitivity of the DRE_{Ghan} to SOA production changes varies between the models. This is connected to how much of the SOA production changes affect the parts of the modelled size distributions where the particles act most efficiently as scatterers of solar radiation. The results from this study show that EC-Earth is the model with most widespread changes of the accumulation and coarse mode particles, and hence largest sensitivity of DRE_{Ghan}. ECHAM is least sensitive here since the SOA changes mostly affect the small particles and are relatively small.

The changes in the CRE_{Ghan} are stronger (up to -0.82 Wm^{-2}) than for the DRE_{Ghan} and more complex. The CRE_{Ghan} changes do not necessarily follow the SOA changes and can be of different sign for different models, and even different regions in the same model. Again, size distribution dynamics are crucial for understanding the sensitivity of the cloud properties and CRE_{Ghan} in the models. Also for the CRE_{Ghan}, ECHAM is the least sensitive model. Overall, the small effects on the size distributions at CCN relevant sizes in this model means that the clouds in ECHAM are virtually unaffected by the sensitivity simulations. The clouds in NorESM are quite strongly affected by the sensitivity simulations, mainly because of shifts in the size distribution. These shifts are mainly a result of changes in condensational growth and thus, the condensation of L/SVOCs is very important for the climate impact of BVOCs in NorESM. EC-Earth is the most sensitive model out of the three models also for the cloud effects. This results from a combination of a size distribution quite sensitive to NPF in combination with low aerosol number concentrations in EC-Earth, which makes the clouds sensitive to aerosol perturbations. Moreover, the NPF in EC-Earth is more sensitive to the ELVOC concentrations than the other models since the BL nucleation rate is calculated from the product of the H_2SO_4 and ELVOC concentrations while the other two models used the sum of the concentrations (see Tab. 1).

We can conclude that the BVOC treatment in the ESMs is of importance and can introduce substantial uncertainties in aerosol climate effects and forcing. There is need for more development and testing of these parameterizations in ESMs ~~, in particular~~ with respect to how the NPF parameterizations affect the size distributions.

Author contributions. M.K.S. performed the model simulations with NorESM. M.K.S and S.M.B did the the data analysis and wrote the manuscript. R.S. performed the model simulations with EC-Earth and wrote parts of the paper. R.M. performed the model simulations with ECHAM and wrote parts of the paper. I.H.H.K. provided support during the setup NorESM. T.v.N., T.B. and D.O. co-developed the EC-Earth version used during the study and provided support for the EC-Earth simulations. M.K.S, S.M.B., R.S., R.M., I.H.K.K. and T.K.B. contributed with discussions regarding the experimental design and data analysis. All contributors have contributed to the discussions regarding the manuscript.

Competing interests. The authors declare that they have no conflict of interest.

Acknowledgements. The research leading to these results has received funding from the European Union's Seventh Framework Programme (FP7/2007-2013) project BACCHUS under grant agreement no 603445. This work was supported by LATICE, a strategic research area funded by the Faculty of Mathematics and Natural Sciences at the University of Oslo. This work has been financed by the research council of Norway (RCN) through the NOTUR/Norstore project NN9485K Biogenic aerosols and climate feedbacks. I.H.H. Karset has been financed by the research council of Norway through the project EVA and the NOTUR/Norstore projects (Sigma2 account: nn2345k, Norstore account: NS2345K). TvN and TB acknowledge funding from the European Union's Horizon 2020 research and innovation programme project CRESCENDO under grant agreement No 641816.

References

Abdul-Razzak, H. and Ghan, S. J.: A parameterization of aerosol activation: 2. Multiple aerosol types, Journal of Geophysical Research: Atmospheres, 105, 6837–6844, https://doi.org/10.1029/1999JD901161, http://doi.wiley.com/10.1029/1999JD901161, 2000.

Albrecht, B. A.: Aerosols, Cloud Microphysics, and Fractional Cloudiness, Science, 245, 1227–1230, https://doi.org/10.1126/science.245.4923.1227, http://science.sciencemag.org/content/245/4923/1227, 1989.

Arneth, A., Niinemets, U., Pressley, S., Back, J., Hari, P., Karl, T., Noe, S., Prentice, I. C., Serca, D., Hickler, T., Wolf, A., and Smith, B.: Process-based estimates of terrestrial ecosystem isoprene emissions: incorporating the effects of a direct CO2-isoprene interaction, Atmospheric Chemistry and Physics, 7, 31–53, https://doi.org/10.5194/acpd-6-8011-2006, 2007.

Bentsen, M., Bethke, I., Debernard, J. B., Iversen, T., Kirkevåg, A., Seland, Ø., Drange, H., Roelandt, C., Seierstad, I. A., Hoose, C., and Kristjánsson, J. E.: The Norwegian Earth System Model, NorESM1-M – Part 1: Description and basic evaluation of the physical climate, Geoscientific Model Development, 6, 687–720, https://doi.org/10.5194/gmd-6-687-2013, http://www.geosci-model-dev.net/6/687/2013/, 2013.

Bonan, G.: Ecological Climatology, Cambridge University Press, 3 edn., 2016.

Carlton, A. G., Pinder, R. W., Bhave, P. V., and Pouliot, G. A.: To What Extent Can Biogenic SOA be Controlled?, Environmental Science & Technology, 44, 3376–3380, https://doi.org/10.1021/es903506b, https://doi.org/10.1021/es903506b, pMID: 20387864, 2010.

Carslaw, K. S., Boucher, O., Spracklen, D. V., Mann, G. W., Rae, J. G. L., Woodward, S., and Kulmala, M.: A review of natural aerosol interactions and feedbacks within the Earth system, Atmospheric Chemistry and Physics, 10, 1701–1737, https://doi.org/10.5194/acp-10-1701-2010, https://www.atmos-chem-phys.net/10/1701/2010/, 2010.

Charlson, R. J., Langner, J., and Rodhe, H.: Sulphate aerosol and climate, Nature, 348, 22, https://doi.org/10.1038/348022a0, https://doi.org/10.1038/348022a0, 1990.

Dee, D. P., Uppala, S. M., Simmons, A. J., Berrisford, P., Poli, P., Kobayashi, S., Andrae, U., Balmaseda, M. A., Balsamo, G., Bauer, P., Bechtold, P., Beljaars, A. C. M., van de Berg, L., Bidlot, J., Bormann, N., Delsol, C., Dragani, R., Fuentes, M., Geer, A. J., Haimberger, L., Healy, S. B., Hersbach, H., Hólm, E. V., Isaksen, L., Kållberg, P., Köhler, M., Matricardi, M., McNally, A. P., Monge-Sanz, B. M., Morcrette, J., Park, B., Peubey, C., de Rosnay, P., Tavolato, C., Thépaut, J., and Vitart, F.: The ERA-Interim reanalysis: configuration and performance of the data assimilation system, Quarterly Journal of the Royal Meteorological Society, 137, 553–597, https://doi.org/10.1002/qj.828, https://rmets.onlinelibrary.wiley.com/doi/abs/10.1002/qj.828, 2011.

Donahue, N. M., Robinson, A. L., Stanier, C. O., and Pandis, S. N.: Coupled Partitioning, Dilution, and Chemical Aging of Semivolatile Organics, Environmental Science & Technology, 40, 2635–2643, https://doi.org/10.1021/es052297c, https://doi.org/10.1021/es052297c, 2006.

Donahue, N. M., Epstein, S. A., Pandis, S. N., and Robinson, A. L.: A two-dimensional volatility basis set: 1. organic-aerosol mixing thermodynamics, Atmospheric Chemistry and Physics, 11, 3303–3318, https://doi.org/https://doi.org/10.5194/acp-11-3303-2011, https://www.atmos-chem-phys.net/11/3303/2011/, 2011.

Dunne, E. M., Gordon, H., Kürten, A., Almeida, J., Duplissy, J., Williamson, C., Ortega, I. K., Pringle, K. J., Adamov, A., Baltensperger, U., Barmet, P., Benduhn, F., Bianchi, F., Breitenlechner, M., Clarke, A., Curtius, J., Dommen, J., Donahue, N. M., Ehrhart, S., Flagan, R. C., Franchin, A., Guida, R., Hakala, J., Hansel, A., Heinritzi, M., Jokinen, T., Kangasluoma, J., Kirkby, J., Kulmala, M., Kupc, A., Lawler, M. J., Lehtipalo, K., Makhmutov, V., Mann, G., Mathot, S., Merikanto, J., Miettinen, P., Nenes, A., Onnela, A., Rap, A., Reddington, C. L. S., Riccobono, F., Richards, N. A. D., Rissanen, M. P., Rondo, L., Sarnela, N., Schobesberger, S., Sengupta, K., Simon, M., Sipilä, M.,

Smith, J. N., Stozkhov, Y., Tomé, A., Tröstl, J., Wagner, P. E., Wimmer, D., Winkler, P. M., Worsnop, D. R., and Carslaw, K. S.: Global atmospheric particle formation from CERN CLOUD measurements, Science, 354, 1119–1124, https://doi.org/10.1126/science.aaf2649, http://science.sciencemag.org/content/354/6316/1119, 2016.

Ehn, M., Thornton, J. A., Kleist, E., Sipilä, M., Junninen, H., Pullinen, I., Springer, M., Rubach, F., Tillmann, R., Lee, B., Lopez-Hilfiker, F., Andres, S., Acir, I.-H., Rissanen, M., Jokinen, T., Schobesberger, S., Kangasluoma, J., Kontkanen, J., Nieminen, T., Kurtén, T., Nielsen, L. B., Jørgensen, S., Kjaergaard, H. G., Canagaratna, M., Maso, M. D., Berndt, T., Petäjä, T., Wahner, A., Kerminen, V.-M., Kulmala, M., Worsnop, D. R., Wildt, J., and Mentel, T. F.: A large source of low-volatility secondary organic aerosol, Nature, 506, 476–479, https://doi.org/10.1038/nature13032, http://www.nature.com/doifinder/10.1038/nature13032, 2014.

Gettelman, A. and Morrison, H.: Advanced Two-Moment Bulk Microphysics for Global Models. Part I: Off-Line Tests and Comparison with Other Schemes, Journal of Climate, 28, 1268–1287, https://doi.org/10.1175/JCLI-D-14-00102.1, https://doi.org/10.1175/JCLI-D-14-00102.1, 2015.

Ghan, S. J.: Technical note: Estimating aerosol effects on cloud radiative forcing, Atmospheric Chemistry and Physics, 13, 9971–9974, https://doi.org/10.5194/acp-13-9971-2013, 2013.

Glasius, M. and Goldstein, A. H.: Recent Discoveries and Future Challenges in Atmospheric Organic Chemistry, Environmental Science & Technology, 50, 2754–2764, https://doi.org/10.1021/acs.est.5b05105, https://doi.org/10.1021/acs.est.5b05105, 2016.

Glasius, M., Hansen, A. M. K., Claeys, M., Henzing, J. S., Jedynska, A. D., Kasper-Giebl, A., Kistler, M., Kristensen, K., Martinsson, J., Maenhaut, W., Nøjgaard, J. K., Spindler, G., Stenström, K. E., Swietlicki, E., Szidat, S., Simpson, D., and Yttri, K. E.: Composition and sources of carbonaceous aerosols in Northern Europe during winter, Atmospheric Environment, 173, 127–141, https://doi.org/10.1016/j.atmosenv.2017.11.005, http://www.sciencedirect.com/science/article/pii/S1352231017307471, 2018.

Gordon, H., Sengupta, K., Rap, A., Duplissy, J., Frege, C., Williamson, C., Heinritzi, M., Simon, M., Yan, C., Almeida, J., Tröstl, J., Nieminen, T., Ortega, I. K., Wagner, R., Dunne, E. M., Adamov, A., Amorim, A., Bernhammer, A.-K., Bianchi, F., Breitenlechner, M., Brilke, S., Chen, X., Craven, J. S., Dias, A., Ehrhart, S., Fischer, L., Flagan, R. C., Franchin, A., Fuchs, C., Guida, R., Hakala, J., Hoyle, C. R., Jokinen, T., Junninen, H., Kangasluoma, J., Kim, J., Kirkby, J., Krapf, M., Kürten, A., Laaksonen, A., Lehtipalo, K., Makhmutov, V., Mathot, S., Molteni, U., Monks, S. A., Onnela, A., Peräkylä, O., Piel, F., Petäjä, T., Praplan, A. P., Pringle, K. J., Richards, N. A. D., Rissanen, M. P., Rondo, L., Sarnela, N., Schobesberger, S., Scott, C. E., Seinfeld, J. H., Sharma, S., Sipilä, M., Steiner, G., Stozhkov, Y., Stratmann, F., Tomé, A., Virtanen, A., Vogel, A. L., Wagner, A. C., Wagner, P. E., Weingartner, E., Wimmer, D., Winkler, P. M., Ye, P., Zhang, X., Hansel, A., Dommen, J., Donahue, N. M., Worsnop, D. R., Baltensperger, U., Kulmala, M., Curtius, J., and Carslaw, K. S.: Reduced anthropogenic aerosol radiative forcing caused by biogenic new particle formation, Proceedings of the National Academy of Sciences, 113, 12 053–12 058, https://doi.org/10.1073/pnas.1602360113, http://www.pnas.org/lookup/doi/10.1073/pnas.1602360113, 2016.

Gordon, H., Kirkby, J., Baltensperger, U., Bianchi, F., Breitenlechner, M., Curtius, J., Dias, A., Dommen, J., Donahue, N. M., Dunne, E. M., Duplissy, J., Ehrhart, S., Flagan, R. C., Frege, C., Fuchs, C., Hansel, A., Hoyle, C. R., Kulmala, M., Kürten, A., Lehtipalo, K., Makhmutov, V., Molteni, U., Rissanen, M. P., Stozkhov, Y., Tröstl, J., Tsagkogeorgas, G., Wagner, R., Williamson, C., Wimmer, D., Winkler, P. M., Yan, C., and Carslaw, K. S.: Causes and importance of new particle formation in the present-day and pre-industrial atmospheres, Journal of Geophysical Research: Atmospheres, pp. 8739–8760, https://doi.org/10.1002/2017JD026844, http://doi.wiley.com/10.1002/2017JD026844, 2017.

Guenther, A. B., Jiang, X., Heald, C. L., Sakulyanontvittaya, T., Duhl, T., Emmons, L. K., and Wang, X.: The model of emissions of gases and aerosols from nature version 2.1 (MEGAN2.1): An extended and updated framework for modeling biogenic emissions, Geoscientific Model Development, 5, 1471–1492, https://doi.org/10.5194/gmd-5-1471-2012, 2012.

Hallquist, M., Wenger, J. C., Baltensperger, U., Rudich, Y., Simpson, D., Claeys, M., Dommen, J., Donahue, N. M., George, C., Goldstein, A. H., Hamilton, J. F., Herrmann, H., Hoffmann, T., Iinuma, Y., Jang, M., Jenkin, M. E., Jimenez, J. L., Kiendler-Scharr, A., Maenhaut, W., McFiggans, G., Mentel, T. F., Monod, A., Prévôt, A. S. H., Seinfeld, J. H., Surratt, J. D., Szmigielski, R., and Wildt, J.: The formation, properties and impact of secondary organic aerosol: current and emerging issues, Atmospheric Chemistry and Physics, 9, 5155–5236, https://doi.org/https://doi.org/10.5194/acp-9-5155-2009, https://www.atmos-chem-phys.net/9/5155/2009/, 2009.

Hantson, S., Knorr, W., Schurgers, G., Pugh, T. A., and Arneth, A.: Global isoprene and monoterpene emissions under changing climate, vegetation, CO2and land use, Atmospheric Environment, 155, 35–45, https://doi.org/10.1016/j.atmosenv.2017.02.010, http://dx.doi.org/10.1016/j.atmosenv.2017.02.010, 2017.

Hazeleger, W., Wang, X., Severijns, C., Ştefănescu, S., Bintanja, R., Sterl, A., Wyser, K., Semmler, T., Yang, S., van den Hurk, B., van Noije, T., van der Linden, E., and van der Wiel, K.: EC-Earth V2.2: description and validation of a new seamless earth system prediction model, Climate Dynamics, 39, 2611–2629, https://doi.org/10.1007/s00382-011-1228-5, http://link.springer.com/10.1007/s00382-011-1228-5, 2012.

Heald, C. L. and Geddes, J. A.: The impact of historical land use change from 1850 to 2000 on secondary particulate matter and ozone, Atmos. Chem. Phys., 16, 14 997–15 010, https://doi.org/10.5194/acp-16-14997-2016, https://www.atmos-chem-phys.net/16/14997/2016/, 2016.

Heald, C. L. and Spracklen, D. V.: Land Use Change Impacts on Air Quality and Climate, Chemical Reviews, 115, 4476–4496, https://doi.org/10.1021/cr500446g, https://doi.org/10.1021/cr500446g, 2015.

IPCC: Summary for Policymakers, in: Climate Change 2013: The Physical Science Basis. Contribution of Working Group I to the Fifth Assessment Report of the Intergovernmental Panel on Climate Change, edited by Stocker, T. F., Qin, D., Plattner, G.-K., Tignor, M., Allen, S. K., Boschung, J., Nauels, A., Xia, Y., Bex, V., and Midgley, P. M., Cambridge University Press, Cambridge, United Kingdom and New York, NY, USA, 2013.

Iversen, T., Bentsen, M., Bethke, I., Debernard, J. B., Kirkevåg, A., Seland, Ø., Drange, H., Kristjansson, J. E., Medhaug, I., Sand, M., and Seierstad, I. A.: The Norwegian Earth System Model, NorESM1-M – Part 2: Climate response and scenario projections, Geoscientific Model Development, 6, 389–415, https://doi.org/10.5194/gmd-6-389-2013, https://www.geosci-model-dev.net/6/389/2013/, 2013.

Jokinen, T., Berndt, T., Makkonen, R., Kerminen, V.-M., Junninen, H., Paasonen, P., Stratmann, F., Herrmann, H., Guenther, A. B., Worsnop, D. R., Kulmala, M., Ehn, M., and Sipilä, M.: Production of extremely low volatile organic compounds from biogenic emissions: Measured yields and atmospheric implications, Proceedings of the National Academy of Sciences, 112, 7123–7128, https://doi.org/10.1073/pnas.1423977112, http://www.pnas.org/lookup/doi/10.1073/pnas.1423977112, 2015.

Kanakidou, M., Tsigaridis, K., Dentener, F. J., and Crutzen, P. J.: Human-activity-enhanced formation of organic aerosols by biogenic hydrocarbon oxidation, Journal of Geophysical Research: Atmospheres, 105, 9243–9354, https://doi.org/10.1029/1999JD901148, https://agupubs.onlinelibrary.wiley.com/doi/abs/10.1029/1999JD901148, 2000.

Karset, I. H. H., Berntsen, T. K., Storelvmo, T., Alterskjær, K., Grini, A., Olivié, D., Kirkevåg, A., Seland, Ø., Iversen, T., and Schulz, M.: Strong impacts on aerosol indirect effects from historical oxidant changes, Atmospheric Chemistry and Physics, 18, 7669–7690, https://doi.org/10.5194/acp-18-7669-2018, https://www.atmos-chem-phys.net/18/7669/2018/, 2018.

Kelly, J. M., Doherty, R. M., O'Connor, F. M., and Mann, G. W.: The impact of biogenic, anthropogenic, and biomass burning volatile organic compound emissions on regional and seasonal variations in secondary organic aerosol, Atmospheric Chemistry and Physics, 18, 7393–7422, https://doi.org/10.5194/acp-18-7393-2018, https://www.atmos-chem-phys.net/18/7393/2018/, 2018.

Kerminen, V. M. and Kulmala, M.: Analytical formulae connecting the 'real' and the 'apparent' nucleation rate and the nuclei number concentration for atmospheric nucleation events, Journal of Aerosol Science, 33, 609–622, https://doi.org/10.1016/S0021-8502(01)00194-X, 2002.

Kirkby, J., Duplissy, J., Sengupta, K., Frege, C., Gordon, H. Williamson, C., Heinritzi, M., Simon, M., Yan, C., Almeida, J., Tröstl, J., Nieminen, Ortega, T., Wagner, R., Adamov, A., Amorim, A., Bernhammer, A., Bianchi, F., Breitenlechner, M., Brilke, S., Chen, X., Craven, J., Dias, A., Ehrhart, S., Flagan, R. C., Franchin, A., Fuchs, C., Guida, R., Hakala, J., Hoyle, C. R., Jokinen, T., Junninen, H. Kangasluoma, J., Kim, J., Krapf, M. Kürten, A., Laaksonen, A., Lehtipalo, K., Makhmutov, V., Mathot, S., Molteni, U., Onnela, A., Peräkylä, O., Piel, F., Petäjä, T., Praplan, A. P., Pringle, K., Rap, A., Richards, N., Riipinen, I., Rissanen, M. P., Rondo, L., Sarnela, N., Schobesberger, S., Scott, C., Seinfeld, J. H., Sipilä, M., Steiner, G., Stozhkov, Y., Stratmann, F., Tomé, A., Virtanen, A., Vogel, A., Wagner, A., Wagner, P., Weingartner, E., Wimmer, D., Winkler, P., Ye, P., Zhang, X., Hansel, A., Dommen, J., Donahue, N. M., Worsnop, D., Baltensperger, U., Kulmala, M., Carslaw, K. S., and Curtius, J.: Ion-induced nucleation of pure biogenic particles, Nature, https://doi.org/10.1038/nature17953, http://dx.doi.org/10.1038/nature17953, 2016.

Kirkevåg, A., Iversen, T., Seland, Ø., Hoose, C., Kristjánsson, J. E., Struthers, H., Ekman, A. M. L., Ghan, S., Griesfeller, J., Nilsson, E. D., and Schulz, M.: Aerosol–climate interactions in the Norwegian Earth System Model – NorESM1-M, Geoscientific Model Development, 6, 207–244, https://doi.org/10.5194/gmd-6-207-2013, http://www.geosci-model-dev.net/6/207/2013/, 2013.

Kirkevåg, A., Grini, A., Olivié, D., Seland, Ø., Alterskjær, K., Hummel, M., Karset, I. H. H., Lewinschal, A., Liu, X., Makkonen, R., Bethke, I., Griesfeller, J., Schulz, M., and Iversen, T.: A production-tagged aerosol module for earth system models, OsloAero5.3 – extensions and updates for CAM5.3-Oslo, Geoscientific Model Development, 11, 13 945–3982, https://doi.org/10.5194/gmd-11-3945-2018, 2018.

Kokkola, H., Hommel, R., Kazil, J., Niemeier, U., Partanen, A.-I., Feichter, J., and Timmreck, C.: Aerosol microphysics modules in the framework of the ECHAM5 climate model ndash; intercomparison under stratospheric conditions, Geoscientific Model Development, 2, 97–112, https://doi.org/10.5194/gmd-2-97-2009, https://www.geosci-model-dev.net/2/97/2009/, 2009.

Kooperman, G. J., Pritchard, M. S., Ghan, S. J., Wang, M., Somerville, R. C. J., and Russell, L. M.: Constraining the influence of natural variability to improve estimates of global aerosol indirect effects in a nudged version of the Community Atmosphere Model 5, Journal of Geophysical Research Atmospheres, 117, 1–16, https://doi.org/10.1029/2012JD018588, 2012.

Kulmala, M., Nieminen, T., Nikandrova, A., Lehtipalo, K., Manninen, H. E., Kajos, M. K., Kolari, P., Lauri, A., Petäjä, T., Krejci, R., Vesala, T., Kerminen, V. M., Nieminen, T., Kolari, P., Hari, P., Bäck, J., Krejci, R., Hansson, H. C., Swietlicki, E., Lindroth, A., Christensen, T. R., and Arneth, A.: CO2-induced terrestrial climate feedback mechanism: From carbon sink to aerosol source and back, Boreal Environment Research, 19, 122–131, 2014.

Lamarque, J.-F., Emmons, L. K., Hess, P. G., Kinnison, D. E., Tilmes, S., Vitt, F., Heald, C. L., Holland, E. A., Lauritzen, P. H., Neu, J., Orlando, J. J., Rasch, P. J., and Tyndall, G. K.: CAM-chem: description and evaluation of interactive atmospheric chemistry in the Community Earth System Model, Geoscientific Model Development, 5, 369–411, https://doi.org/10.5194/gmd-5-369-2012, https://www.geosci-model-dev.net/5/369/2012/, 2012.

Lehtinen, K. E., Dal Maso, M., Kulmala, M., and Kerminen, V. M.: Estimating nucleation rates from apparent particle formation rates and vice versa: Revised formulation of the Kerminen-Kulmala equation, Journal of Aerosol Science, 38, 988–994, https://doi.org/10.1016/j.jaerosci.2007.06.009, 2007.

Lin, G., Wan, H., Zhang, K., Qian, Y., and Ghan, S. J.: Can nudging be used to quantify model sensitivities in precipitation and cloud forcing?, Journal of Advances in Modeling Earth Systems, 8, 1073–1091, https://doi.org/10.1002/2016MS000659, https://agupubs.onlinelibrary.wiley.com/doi/abs/10.1002/2016MS000659, 2016.

Lohmann, U. and Hoose, C.: Sensitivity studies of different aerosol indirect effects in mixed-phase clouds, Atmospheric Chemistry and Physics, 9, 8917–8934, https://doi.org/10.5194/acp-9-8917-2009, https://www.atmos-chem-phys.net/9/8917/2009/, 2009.

Makkonen, R., Asmi, A., Kerminen, V.-M., Boy, M., Arneth, A., Guenther, A., and Kulmala, M.: BVOC-aerosol-climate interactions in the global aerosol-climate model ECHAM5.5-HAM2, Atmospheric Chemistry and Physics, 12, 10 077–10 096, https://doi.org/10.5194/acp-12-10077-2012, 2012.

Makkonen, R., Seland, O., Kirkevåg, A., Iversen, T., and Kristjansson, J. E.: Evaluation of aerosol number concentrations in NorESM with improved nucleation parameterization, Atmospheric Chemistry and Physics, 14, 5127–5152, https://doi.org/10.5194/acp-14-5127-2014, 2014.

Morrison, H. and Gettelman, A.: A new two-moment bulk stratiform cloud microphysics scheme in the community atmosphere model, version 3 (CAM3). Part I: Description and numerical tests, Journal of Climate, 21, 3642–3659, https://doi.org/10.1175/2008JCLI2105.1, 2008.

Neale, R. B., Gettelman, A., Park, S., Chen, C.-c., Lauritzen, P. H., Williamson, D. L., Conley, A. J., Kinnison, D., Marsh, D., Smith, A. K., Vitt, F., Garcia, R., Lamarque, J.-f., Mills, M., Tilmes, S., Morrison, H., Cameron-smith, P., Collins, W. D., Iacono, M. J., Easter, R. C., Liu, X., Ghan, S. J., Rasch, P. J., and Taylor, M. a.: Description of the NCAR Community Atmosphere Model (CAM 5.0). NCAR Technical Notes., Ncar/Tn-464+Str, p. 214, https://doi.org/10.5065/D6N877R0., 2012.

Oleson, K. W., Lawrence, D. M., Bonan, G. B., Drewniak, B., Huang, M., Koven, C. D., Levis, S., Li, F., Riley, W. J., Subin, Z. M., Swenson, S. C., Thornton, P. E., Bozbiyik, A., Fisher, R., Heald, C. L., Kluzek, E., Lamarque, J.-f., Lawrence, P. J., Leung, L. R., Lipscomb, W., Muszala, S., Ricciuto, D. M., Sacks, W., Sun, Y., Tang, J., and Yang, Z.-L.: Technical description of version 4.0 of the Community Land Model (CLM), NCAR/TN-503+STR NCAR Technical Note, p. 266, http://citeseerx.ist.psu.edu/viewdoc/summary?doi=10.1.1.172.7769{%}5Cnpapers3://publication/uuid/E8E12D50-5C26-4DF4-A67C-753D8AC5D002, 2013.

Paasonen, P., Nieminen, T., Asmi, E., Manninen, H. E., Petäjä, T., Plass-Dülmer, C., Flentje, H., Birmili, W., Wiedensohler, A., Hõrrak, U., Metzger, A., Hamed, A., Laaksonen, A., Facchini, M. C., Kerminen, V. M., and Kulmala, M.: On the roles of sulphuric acid and low-volatility organic vapours in the initial steps of atmospheric new particle formation, Atmospheric Chemistry and Physics, 10, 11 223–11 242, https://doi.org/10.5194/acp-10-11223-2010, 2010.

Paasonen, P., Asmi, A., Petäjä, T., Kajos, M. K., Äijälä, M., Junninen, H., Holst, T., Abbatt, J. P. D., Arneth, A., Birmili, W., van der Gon, H. D., Hamed, A., Hoffer, A., Laakso, L., Laaksonen, A., Richard Leaitch, W., Plass-Dülmer, C., Pryor, S. C., Räisänen, P., Swietlicki, E., Wiedensohler, A., Worsnop, D. R., Kerminen, V.-M., and Kulmala, M.: Warming-induced increase in aerosol number concentration likely to moderate climate change, Nature Geoscience, 6, 438–442, https://doi.org/10.1038/ngeo1800, http://www.nature.com/doifinder/10.1038/ngeo1800, 2013.

Park, S. and Bretherton, C. S.: The University of Washington Shallow Convection and Moist Turbulence Schemes and Their Impact on Climate Simulations with the Community Atmosphere Model, Journal of Climate, 22, 3449–3469, https://doi.org/10.1175/2008JCLI2557.1, https://doi.org/10.1175/2008JCLI2557.1, 2009.

Riccobono, F., Schobesberger, S., Scott, C. E., Dommen, J., Ortega, I. K., Rondo, L., Almeida, J., Amorim, A., Bianchi, F., Breitenlechner, M., David, A., Downard, A., Dunne, E. M., Duplissy, J., Ehrhart, S., Flagan, R. C., Franchin, A., Hansel, A., Junninen, H., Kajos, M., Keskinen, H., Kupc, A., Kürten, A., Kvashin, A. N., Laaksonen, A., Lehtipalo, K., Makhmutov, V., Mathot, S., Nieminen, T., Onnela, A.,

Petäjä, T., Praplan, A. P., Santos, F. D., Schallhart, S., Seinfeld, J. H., Sipilä, M., Spracklen, D. V., Stozhkov, Y., Stratmann, F., Tomé, A., Tsagkogeorgas, G., Vaattovaara, P., Viisanen, Y., Vrtala, A., Wagner, P. E., Weingartner, E., Wex, H., Wimmer, D., Carslaw, K. S., Curtius, J., Donahue, N. M., Kirkby, J., Kulmala, M., Worsnop, D. R., and Baltensperger, U.: Oxidation Products of Biogenic Emissions Contribute to Nucleation of Atmospheric Particles, Science, 344, 717–721, https://doi.org/10.1126/science.1243527, http://science.sciencemag.org/content/344/6185/717, 2014.

Riipinen, I., Pierce, J. R., Yli-Juuti, T., Nieminen, T., Häkkinen, S., Ehn, M., Junninen, H., Lehtipalo, K., Petäjä, T., Slowik, J., Chang, R., Shantz, N. C., Abbatt, J., Leaitch, W. R., Kerminen, V.-M., Worsnop, D. R., Pandis, S. N., Donahue, N. M., and Kulmala, M.: Organic condensation: a vital link connecting aerosol formation to cloud condensation nuclei (CCN) concentrations, Atmos. Chem. Phys., 11, 3865–3878, https://doi.org/10.5194/acp-11-3865-2011, http://www.atmos-chem-phys.net/11/3865/2011/, 2011.

Riipinen, I., Yli-Juuti, T., Pierce, J. R., Petaja, T., Worsnop, D. R., Kulmala, M., and Donahue, N. M.: The contribution of organics to atmospheric nanoparticle growth, Nature Geosci, https://doi.org/10.1038/ngeo1499, http://dx.doi.org/10.1038/ngeo1499, 2012.

Scott, C. E., Monks, S. A., Spracklen, D. V., Arnold, S. R., Forster, P. M., Rap, A., Carslaw, K. S., Chipperfield, M. P., Reddington, C. L. S., and Wilson, C.: Impact on short-lived climate forcers (SLCFs) from a realistic land-use change scenario via changes in biogenic emissions, Faraday Discussions, 200, 101–120, https://doi.org/10.1039/c7fd00028f, 2017.

Scott, C. E., Monks, S. A., Spracklen, D. V., Arnold, S. R., Forster, P. M., Rap, A., Äijälä, M., Artaxo, P., Carslaw, K. S., Chipperfield, M. P., Ehn, M., Gilardoni, S., Heikkinen, L., Kulmala, M., Petäjä, T., Reddington, C. L. S., Rizzo, L. V., Swietlicki, E., Vignati, E., and Wilson, C.: Impact on short-lived climate forcers increases projected warming due to deforestation, Nature Communications, 9, 157, https://doi.org/10.1038/s41467-017-02412-4, https://www.nature.com/articles/s41467-017-02412-4, 2018.

Shrivastava, M., Easter, R. C., Liu, X., Zelenyuk, A., Singh, B., Zhang, K., Ma, P. L., Chand, D., Ghan, S., Jimenez, J. L., Zhang, Q., Fast, J., Rasch, P. J., and Tiitta, P.: Global transformation and fate of SOA: Implications of low-volatility SOA and gas-phase fragmentation reactions, Journal of Geophysical Research Atmospheres, 120, 4169–4195, https://doi.org/10.1002/2014JD022563, 2015.

Shrivastava, M., Cappa, C. D., Fan, J., Goldstein, A. H., Guenther, A. B., Jimenez, J. L., Kuang, C., Laskin, A., Martin, S. T., Ng, N. L., Petaja, T., Pierce, J. R., Rasch, P. J., Roldin, P., Seinfeld, J. H., Shilling, J., Smith, J. N., Thornton, J. A., Volkamer, R., Wang, J., Worsnop, D. R., Zaveri, R. A., Zelenyuk, A., and Zhang, Q.: Recent advances in understanding secondary organic aerosol: Implications for global climate forcing, Reviews of Geophysics, 55, 509–559, https://doi.org/10.1002/2016RG000540, 2017.

Sindelarova, K., Granier, C., Bouarar, I., Guenther, A., Tilmes, S., Stavrakou, T., Müller, J. F., Kuhn, U., Stefani, P., and Knorr, W.: Global data set of biogenic VOC emissions calculated by the MEGAN model over the last 30 years, Atmospheric Chemistry and Physics, 14, 9317–9341, https://doi.org/10.5194/acp-14-9317-2014, 2014.

Sporre, M. K., Blichner, S. M., Karset, I. H. H., Makkonen, R., and Berntsen, T. K.: BVOC–aerosol–climate feedbacks investigated using NorESM, Atmospheric Chemistry and Physics, 19, 4763–4782, https://doi.org/10.5194/acp-19-4763-2019, https://www.atmos-chem-phys.net/19/4763/2019/, 2019.

Spracklen, D. V. and Rap, A.: Natural aerosol–climate feedbacks suppressed by anthropogenic aerosol, Geophysical Research Letters, 40, 5316–5319, https://doi.org/10.1002/2013GL057966, http://dx.doi.org/10.1002/2013GL057966, 2013.

Spracklen, D. V., Carslaw, K. S., Kulmala, M., Kerminen, V.-M., Mann, G. W., and Sihto, S.-L.: The contribution of boundary layer nucleation events to total particle concentrations on regional and global scales, Atmospheric Chemistry and Physics, 6, 5631–5648, https://doi.org/10.5194/acp-6-5631-2006, https://www.atmos-chem-phys.net/6/5631/2006/, 2006.

Spracklen, D. V., Jimenez, J. L., Carslaw, K. S., Worsnop, D. R., Evans, M. J., Mann, G. W., Zhang, Q., Canagaratna, M. R., Allan, J., Coe, H., McFiggans, G., Rap, A., and Forster, P.: Aerosol mass spectrometer constraint on the global secondary organic aerosol budget,

Atmospheric Chemistry and Physics, 11, 12 109–12 136, https://doi.org/10.5194/acp-11-12109-2011, https://www.atmos-chem-phys.net/11/12109/2011/, 2011.

Stier, P., Feichter, J., Kinne, S., Kloster, S., Vignati, E., Wilson, J., Ganzeveld, L., Tegen, I., Werner, M., Balkanski, Y., Schulz, M., Boucher, O., Minikin, A., and Petzold, A.: The aerosol-climate model ECHAM5-HAM, Atmospheric Chemistry and Physics, 5, 1125–1156, https://doi.org/10.5194/acp-5-1125-2005, https://www.atmos-chem-phys.net/5/1125/2005/, 2005.

Tröstl, J., Chuang, W. K., Gordon, H., Heinritzi, M., Yan, C., Molteni, U., Ahlm, L., Frege, C., Bianchi, F., Wagner, R., Simon, M., Lehtipalo, K., Williamson, C., Craven, J. S., Duplissy, J., Adamov, A., Almeida, J., Bernhammer, A.-K., Breitenlechner, M., Brilke, S., Dias, A., Ehrhart, S., Flagan, R. C., Franchin, A., Fuchs, C., Guida, R., Gysel, M., Hansel, A., Hoyle, C. R., Jokinen, T., Junninen, H., Kangasluoma, J., Keskinen, H., Kim, J., Krapf, M., Kürten, A., Laaksonen, A., Lawler, M., Leiminger, M., Mathot, S., Möhler, O., Nieminen, T., Onnela, A., Petäjä, T., Piel, F. M., Miettinen, P., Rissanen, M. P., Rondo, L., Sarnela, N., Schobesberger, S., Sengupta, K., Sipilä, M., Smith, J. N., Steiner, G., Tomè, A., Virtanen, A., Wagner, A. C., Weingartner, E., Wimmer, D., Winkler, P. M., Ye, P., Carslaw, K. S., Curtius, J., Dommen, J., Kirkby, J., Kulmala, M., Riipinen, I., Worsnop, D. R., Donahue, N. M., and Baltensperger, U.: The role of low-volatility organic compounds in initial particle growth in the atmosphere, Nature, 533, 527–531, https://doi.org/10.1038/nature18271, http://www.nature.com/doifinder/10.1038/nature18271, 2016.

Tsigaridis, K. and Kanakidou, M.: The Present and Future of Secondary Organic Aerosol Direct Forcing on Climate, Current Climate Change Reports, 4, 1–15, https://doi.org/10.1007/s40641-018-0092-3, http://link.springer.com/10.1007/s40641-018-0092-3, 2018.

Tsigaridis, K., Daskalakis, N., Kanakidou, M., Adams, P. J., Artaxo, P., Bahadur, R., Balkanski, Y., Bauer, S. E., Bellouin, N., Benedetti, A., Bergman, T., Berntsen, T. K., Beukes, J. P., Bian, H., Carslaw, K. S., Chin, M., Curci, G., Diehl, T., Easter, R. C., Ghan, S. J., Gong, S. L., Hodzic, A., Hoyle, C. R., Iversen, T., Jathar, S., Jimenez, J. L., Kaiser, J. W., Kirkevåg, A., Koch, D., Kokkola, H., Lee, Y. H., Lin, G., Liu, X., Luo, G., Ma, X., Mann, G. W., Mihalopoulos, N., Morcrette, J.-J., Müller, J.-F., Myhre, G., Myriokefalitakis, S., Ng, N. L., O'Donnell, D., Penner, J. E., Pozzoli, L., Pringle, K. J., Russell, L. M., Schulz, M., Sciare, J., Seland, Ø., Shindell, D. T., Sillman, S., Skeie, R. B., Spracklen, D., Stavrakou, T., Steenrod, S. D., Takemura, T., Tiitta, P., Tilmes, S., Tost, H., van Noije, T., van Zyl, P. G., von Salzen, K., Yu, F., Wang, Z., Wang, Z., Zaveri, R. A., Zhang, H., Zhang, K., Zhang, Q., and Zhang, X.: The AeroCom evaluation and intercomparison of organic aerosol in global models, Atmospheric Chemistry and Physics, 14, 10 845–10 895, https://doi.org/10.5194/acp-14-10845-2014, https://www.atmos-chem-phys.net/14/10845/2014/, 2014a.

Tsigaridis, K., Daskalakis, N., Kanakidou, M., Adams, P. J., Artaxo, P., Bahadur, R., Balkanski, Y., Bauer, S. E., Bellouin, N., Benedetti, A., Bergman, T., Berntsen, T. K., Beukes, J. P., Bian, H., Carslaw, K. S., Chin, M., Curci, G., Diehl, T., Easter, R. C., Ghan, S. J., Gong, S. L., Hodzic, A., Hoyle, C. R., Iversen, T., Jathar, S., Jimenez, J. L., Kaiser, J. W., Kirkevåg, A., Koch, D., Kokkola, H., Lee, Y. H., Lin, G., Liu, X., Luo, G., Ma, X., Mann, G. W., Mihalopoulos, N., Morcrette, J.-J., Müller, J.-F., Myhre, G., Myriokefalitakis, S., Ng, N. L., O'Donnell, D., Penner, J. E., Pozzoli, L., Pringle, K. J., Russell, L. M., Schulz, M., Sciare, J., Seland, , Shindell, D. T., Sillman, S., Skeie, R. B., Spracklen, D., Stavrakou, T., Steenrod, S. D., Takemura, T., Tiitta, P., Tilmes, S., Tost, H., van Noije, T., van Zyl, P. G., von Salzen, K., Yu, F., Wang, Z., Wang, Z., Zaveri, R. A., Zhang, H., Zhang, K., Zhang, Q., and Zhang, X.: The AeroCom evaluation and intercomparison of organic aerosol in global models, Atmos. Chem. Phys., 14, 10 845–10 895, https://doi.org/10.5194/acp-14-10845-2014, https://www.atmos-chem-phys.net/14/10845/2014/, 2014b.

Twomey, S.: Pollution and the Planetary Albedo, Atmospheric Environment, 8, 1251–1256, 1974.

Unger, N.: On the role of plant volatiles in anthropogenic global climate change, Geophysical Research Letters, 41, 8563–8569, https://doi.org/10.1002/2014GL061616, https://agupubs.onlinelibrary.wiley.com/doi/abs/10.1002/2014GL061616, 2014.

van Noije, T. P. C., Le Sager, P., Segers, A. J., van Velthoven, P. F. J., Krol, M. C., Hazeleger, W., Williams, A. G., and Chambers, S. D.: Simulation of tropospheric chemistry and aerosols with the climate model EC-Earth, Geoscientific Model Development, 7, 2435–2475, https://doi.org/10.5194/gmd-7-2435-2014, https://www.geosci-model-dev.net/7/2435/2014/, 2014.

Vehkamäki, H., Kulmala, M., Napari, I., Lehtinen, K. E. J., Timmreck, C., Noppel, M., and Laaksonen, A.: An improved parameterization for sulfuric acid–water nucleation rates for tropospheric and stratospheric conditions, Journal of Geophysical Research, 107, 4622, https://doi.org/10.1029/2002JD002184, http://doi.wiley.com/10.1029/2002JD002184, 2002.

Vignati, E., Wilson, J., and Stier, P.: M7: An efficient size-resolved aerosol microphysics module for large-scale aerosol transport models, Journal of Geophysical Research: Atmospheres, 109, https://doi.org/10.1029/2003JD004485, https://agupubs.onlinelibrary.wiley.com/doi/abs/10.1029/2003JD004485, 2004.

Williams, J. E., Strunk, A., Huijnen, V., and van Weele, M.: The application of the Modified Band Approach for the calculation of on-line photodissociation rate constants in TM5: implications for oxidative capacity, Geoscientific Model Development, 5, 15–35, https://doi.org/10.5194/gmd-5-15-2012, https://www.geosci-model-dev.net/5/15/2012/, 2012.

Williams, J. E., Boersma, K. F., Le Sager, P., and Verstraeten, W. W.: The high-resolution version of TM5-MP for optimized satellite retrievals: description and validation, Geoscientific Model Development, 10, 721–750, https://doi.org/10.5194/gmd-10-721-2017, https://www.geosci-model-dev.net/10/721/2017/, 2017.

Yu, F.: A secondary organic aerosol formation model considering successive oxidation aging and kinetic condensation of organic compounds: global scale implications, Atmos. Chem. Phys., 11, 1083–1099, https://doi.org/10.5194/acp-11-1083-2011, https://www.atmos-chem-phys.net/11/1083/2011/, 2011.

Zhang, G. J. and McFarlane, N. A.: Sensitivity of climate simulations to the parameterization of cumulus convection in the Canadian climate centre general circulation model, Atmosphere-Ocean, 33, 407–446, https://doi.org/10.1080/07055900.1995.9649539, http://dx.doi.org/10.1080/07055900.1995.9649539, 1995.

Zhang, K., O'Donnell, D., Kazil, J., Stier, P., Kinne, S., Lohmann, U., Ferrachat, S., Croft, B., Quaas, J., Wan, H., Rast, S., and Feichter, J.: The global aerosol-climate model ECHAM-HAM, version 2: sensitivity to improvements in process representations, Atmospheric Chemistry and Physics, 12, 8911–8949, https://doi.org/10.5194/acp-12-8911-2012, https://www.atmos-chem-phys.net/12/8911/2012/, 2012a.

Zhang, Q., Jimenez, J. L., Canagaratna, M. R., Allan, J. D., Coe, H., Ulbrich, I., Alfarra, M. R., Takami, A., Middlebrook, A. M., Sun, Y. L., Dzepina, K., Dunlea, E., Docherty, K., DeCarlo, P. F., Salcedo, D., Onasch, T., Jayne, J. T., Miyoshi, T., Shimono, A., Hatakeyama, S., Takegawa, N., Kondo, Y., Schneider, J., Drewnick, F., Borrmann, S., Weimer, S., Demerjian, K., Williams, P., Bower, K., Bahreini, R., Cottrell, L., Griffin, R. J., Rautiainen, J., Sun, J. Y., Zhang, Y. M., and Worsnop, D. R.: Ubiquity and dominance of oxygenated species in organic aerosols in anthropogenically-influenced Northern Hemisphere midlatitudes, Geophysical Research Letters, 34, https://doi.org/10.1029/2007GL029979, https://agupubs.onlinelibrary.wiley.com/doi/abs/10.1029/2007GL029979, 2007.

Zhang, R., Khalizov, A., Wang, L., Hu, M., and Xu, W.: Nucleation and Growth of Nanoparticles in the Atmosphere, Chemical Reviews, 112, 1957–2011, https://doi.org/10.1021/cr2001756, http://dx.doi.org/10.1021/cr2001756, 2012b.

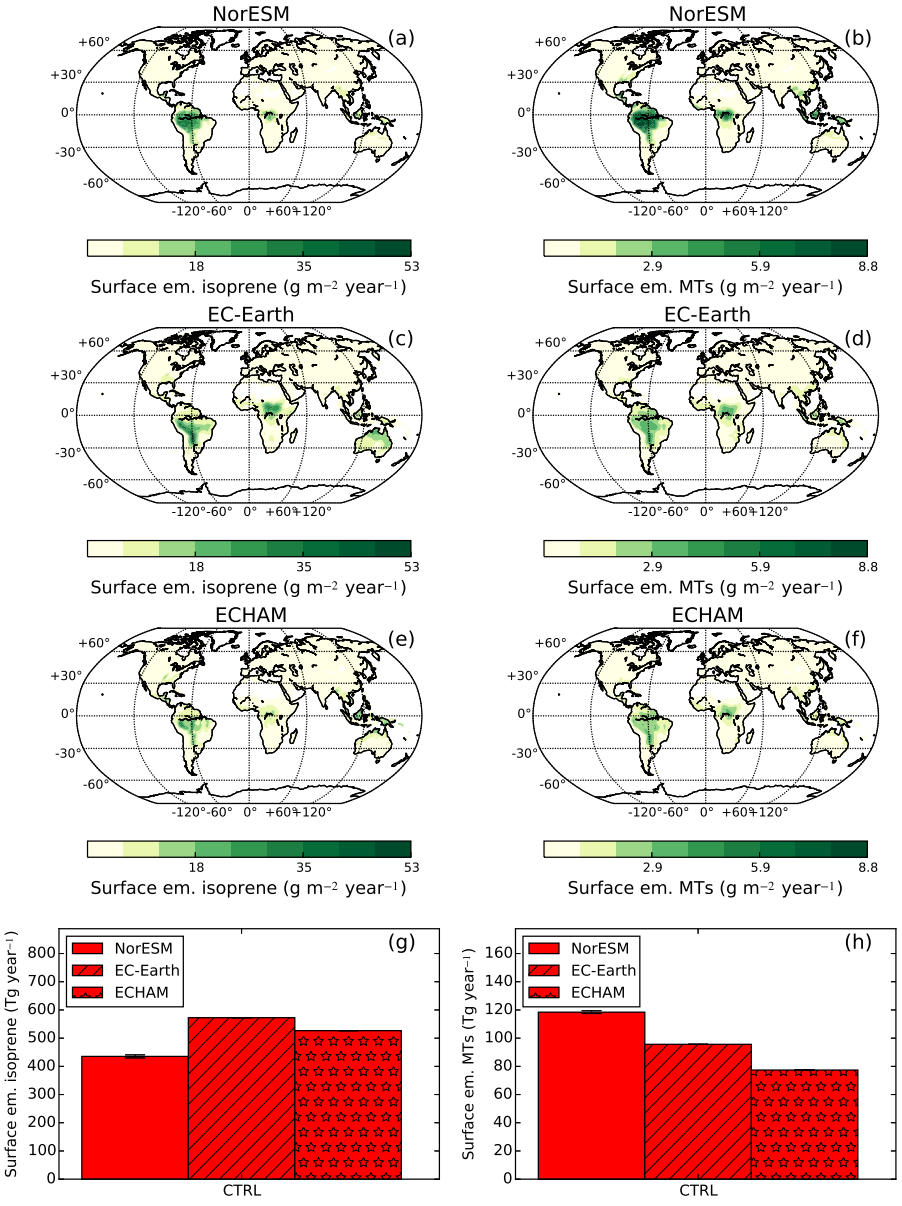

Figure 1. Maps of annually averaged surface emissions of isoprene (a,c and e) and monoterpenes (MTs) (b,d and f) for NorESM, EC-Earth and ECHAM. ECHAM and EC-Earth uses prescribed emissions and there are therefore no error bars presented for these models. Also shown are the global yearly surface emissions of isoprene (g) and MTs (h). The error bars denote the standard error of mean of the yearly averages.

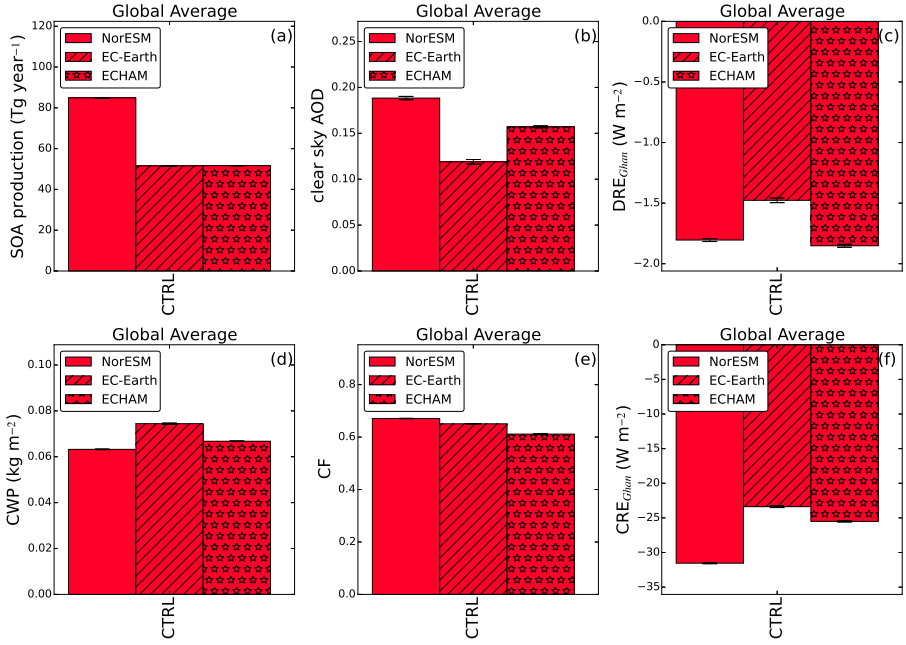

Figure 2. Bar plot of the total yearly global SOA production and the yearly averaged aerosol optical depth (AOD), direct radiative effect (DRE$_{Ghan}$), cloud water path (CWP), cloud fraction (CF) and cloud radiative effect (CRE$_{Ghan}$) for all three models for the *CTRL* experiment. The error bars denote the standard error of mean of the yearly averages.

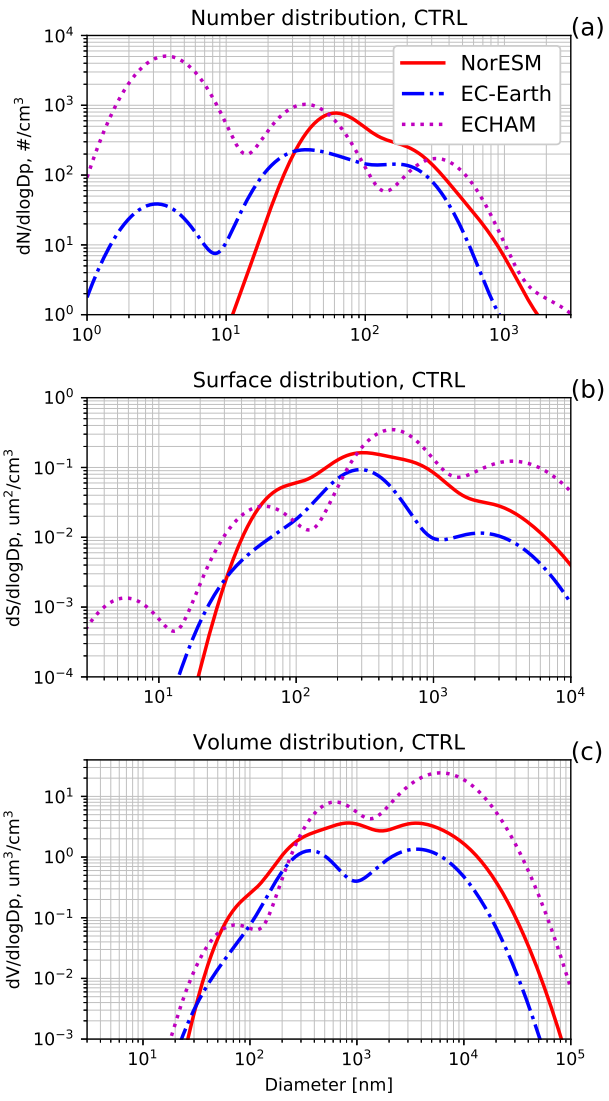

Figure 3. Globally averaged aerosol number size distributions (a), surface size distributions (b) and volume size distributions from the three models from the *CTRL* simulation. The diameters are the dry diameters. Note the different scales on the x-axis in the subplots.

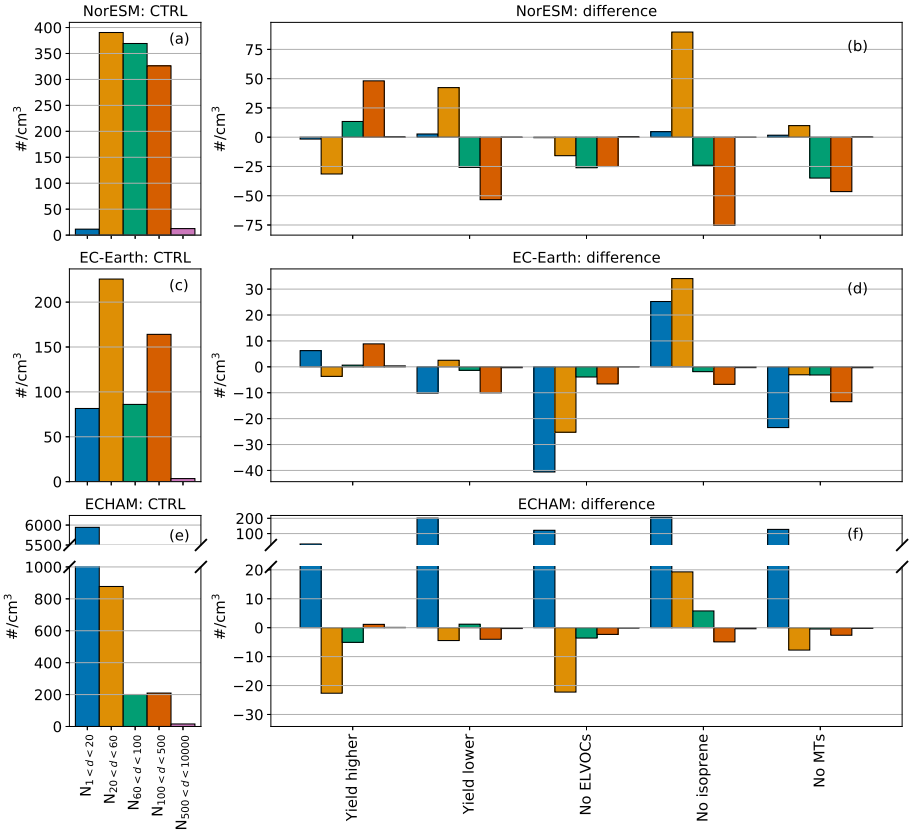

Figure 4. Bar plots of the number concentration of particles of selected sizes. In a, c and e the number concentrations from the *CTRL* simulations are shown. In b, d and f the absolute differences between the sensitivity simulations and the control simulations are shown for each size bin. Note that there are different scales used for the different models.

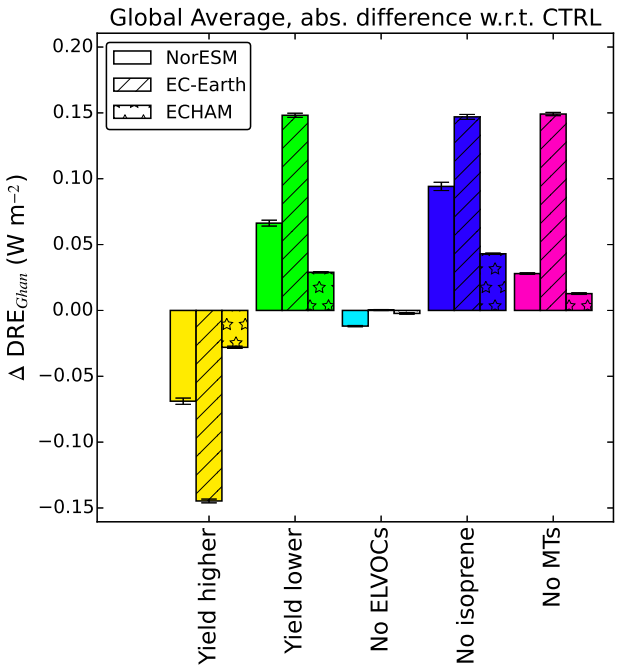

Figure 5. Bar plot of the average direct radiative effect (DRE$_{Ghan}$) difference between each sensitivity simulation and the *CTRL* simulations. Coloured bars indicate a significant difference in the simulation averages with a 95% confidence interval. The error bars denote the standard error of mean of the yearly differences.

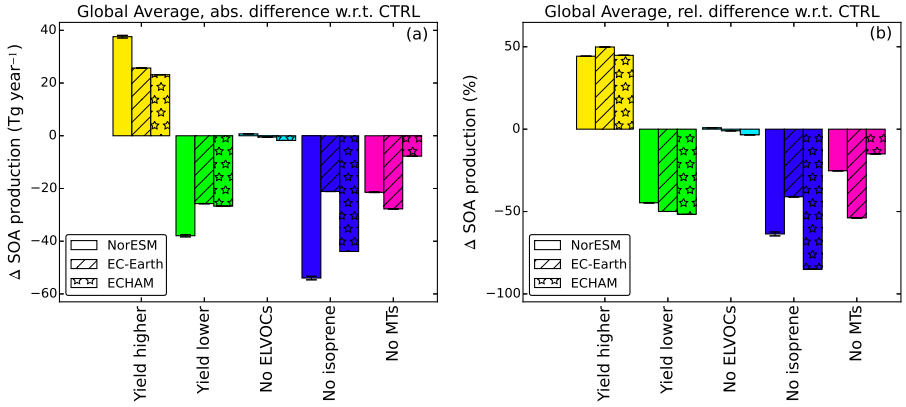

Figure 6. Bar plot of the average yearly SOA production changes in the three models. In (a), the absolute difference between each sensitivity simulation and the *CTRL* simulations are shown and in (b) the relative differences between the sensitivity simulations and the control simulations are shown for all three models. Coloured bars indicate a significant difference in the simulation averages with a 95% confidence interval. The error bars denote the standard error of mean of the yearly differences.

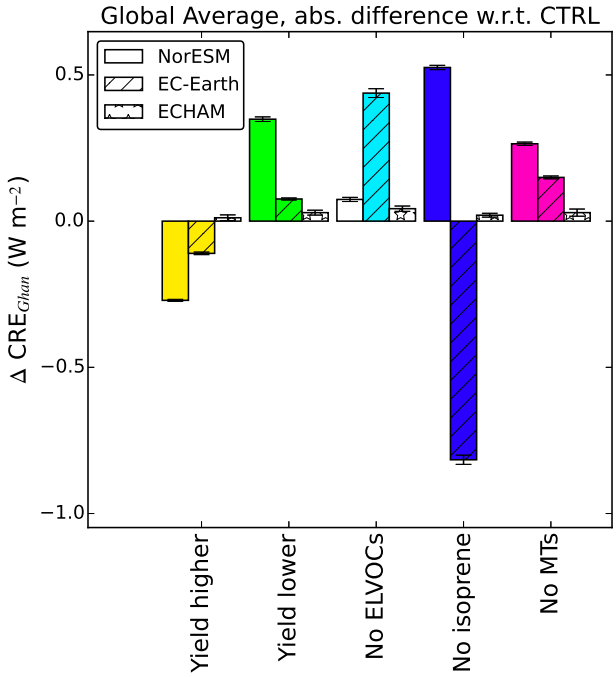

Figure 7. Bar plot of the global average cloud radiative effect (CRE$_{Ghan}$) between each sensitivity simulation and the *CTRL* simulations. Coloured bars indicate a significant difference in the simulation averages with a 95% confidence interval. The error bars denote the standard error of mean of the yearly differences.

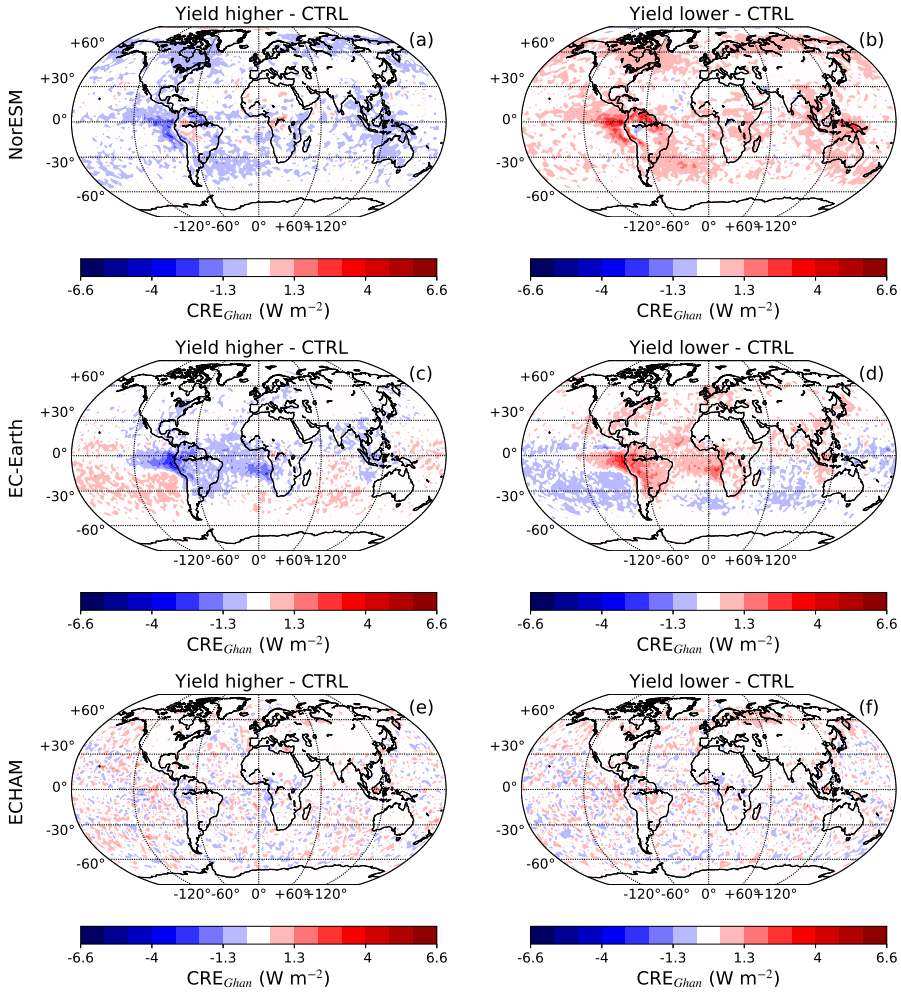

Figure 8. Maps of the difference in the average cloud radiative effect (CRE_{Ghan}) between the *Yield higher* (a,c and d) and *Yield lower* (b, d and h) with respect to the *CTRL simulation*. This is shown for NorESM (a and b), EC-Earth (c and d) and ECHAM (e and f).

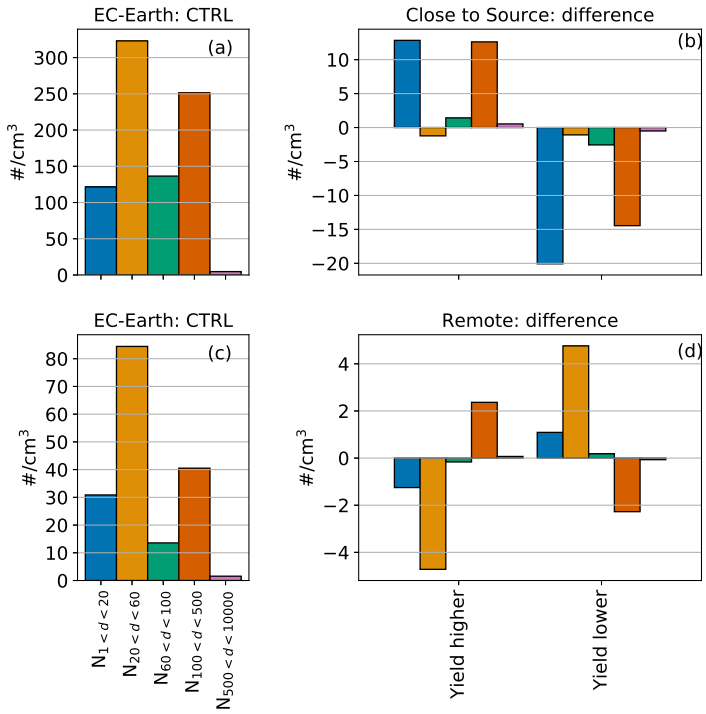

Figure 9. Bar plots of the number concentration of particles of selected sizes ranges for EC-Earth, close to and far away from the sources. In a and c the number concentrations from the *CTRL* simulations are shown. In b and d the differences between the sensitivity simulations and the *CTRL* simulations are shown for each size bin. Note that there are different scales used for the different regions. The areas defined as close and remote are based on changes in CCN concentrations (positive or negative) at 1 % supersaturation. These areas can be seen in Fig. S21.

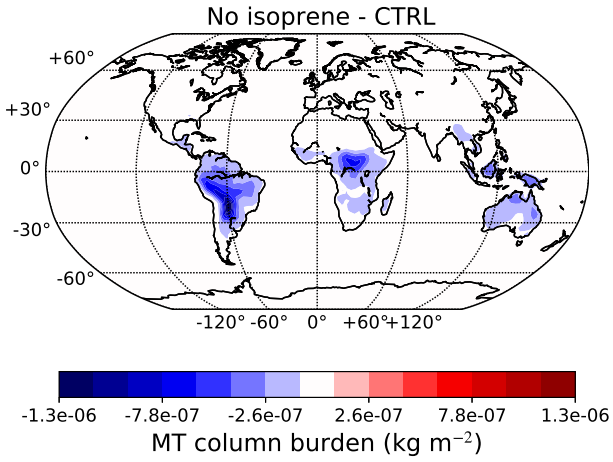

Figure 10. Map of the difference in the average MT column burden between the *No isoprene* and *CTRL* simulation for EC-Earth.

Table 1. This Table lists similarities and dissimilarities between the three ESM of particularly relevance for this study.

Properties	NorESM	EC-Earth	ECHAM
Aerosol model	OsloAero	M7	M7
BVOC emissions	MEGAN v2.1 interactive	MEGAN-MACC prescribed	MEGAN-MACC prescribed
Oxidant fields	Prescribed	Interactive	Prescribed
Oxidised BVOC Tracers	ELVOC / L/SVOC	ELVOC / L/SVOC	ELVOC / L/SVOC
ELVOC formed from	MTs	isoprene and MTs	isoprene and MTs
Binary nucl. param.	Vehkamäki et al. (2002)	Vehkamäki et al. (2002)	Vehkamäki et al. (2002)
BL nucleation rate J =	$A_1[H_2SO_4] + A_2$[ELVOC]	$A_3[H_2SO_4]^2$ x [ELVOC]	$A_1[H_2SO_4] + A_2$[ELVOC]
Cloud activation scheme	Abdul-Razzak and Ghan (2000)	Abdul-Razzak and Ghan (2000)	Abdul-Razzak and Ghan (2000)

$A_1 = 6.1 \times 10^{-7}$ s^{-1}
$A_2 = 3.9 \times 10^{-8}$ s^{-1}
$A_3 = 3.27 \times 10^{-21}$ cm^{-6} s^{-1}

Table 2. Yields and resulting products from the reactions of BVOCs with oxidants to form ELVOC and L/SVOC for the three ESMs. In ECHAM, there are different yields for endocyclic MTs and the other MTs. The equations for the endocyclic MTs are written separately and the other MTs are shown on the same rows as the MTs in the other models.

Model	NorESM	EC-Earth	ECHAM
Isop. + OH	0.05 L/SVOC	0.0097 L/SVOC + 0.0003 ELVOC	0.0482 L/SVOC + 0.0018 ELVOC
Isop. + O_3	0.05 L/SVOC	0.0099 L/SVOC + 0.0001 ELVOC	0.0498 L/SVOC + 0.00016 ELVOC
Isop. + NO_3	0.05 L/SVOC	-	-
MTs + OH	0.15 L/SVOC	0.14 L/SVOC + 0.01 ELVOC	0.14 L/SVOC + 0.01 ELVOC
MTs + O_3	0.15 ELVOC	0.1 L/SVOC + 0.05 ELVOC	0.147 L/SVOC + 0.003 ELVOC
MTs + NO_3	0.15 L/SVOC	-	-
Endocyclic MTs + OH	-	-	0.145 L/SVOC + 0.005 ELVOC
Endocyclic MTs + O_3	-	-	0.1 L/SVOC + 0.05 ELVOC